



Invited Paper

Coherent optical frequency combs: From principles to applications



Hao Zhang^{a,1}, Bing Chang^{a,1}, Zhaoyu Li^a, Yu-Pei Liang^a, Chen-Ye Qin^a,
Chun Wang^{a,b}, Han-Ding Xia^b, Teng Tan^{a,*}, Bai-Cheng Yao^{a,**}

^aKey Laboratory of Optical Fiber Sensing and Communications, University of Electronic Science and Technology of China, Chengdu, 611731, China

^bResearch Center of Laser Fusion, China Academy of Engineering Physics, Mianyang, 621900, China

ARTICLE INFO

Publishing editor: Yu-Lian He

Index Terms:

Microcavity

Nonlinear optics

Optical frequency comb

Soliton

ABSTRACT

A coherent optical frequency comb is a kind of broad-spectrum light sources delivering equidistant frequencies, and correspondingly its temporal waveform appears as a sequence of ultrashort pulses. Being the cornerstone technology of today's laser and time-frequency disciplines, it effectively links the optical frequency and the microwave frequency, and has promoted the development of diverse applications, such as precision spectroscopy, optical measurement, coherent optical communications, and optical clocks in the past two decades. In this review, we comprehensively introduce the development path, physical principle, generation/tuning methods, and advanced applications of optical frequency combs.

1. Introduction

An optical frequency comb (OFC) is a light source whose spectrum consists of discrete longitude modes with equidistant comb lines. Following the advent of ultrashort pulse lasers, OFC has become another striking breakthrough in the field of the laser technology. OFC was first proposed in the study of mode-locked lasers in the 1970s [1]. In 1978, Eckstein, Ferguson, and Hänsch [2] determined a new value of the fine-structure splitting and verified that the longitudinal mode of the mode-locked laser was composed of "comb line" in the frequency domain, which means that ultrashort laser pulses can be used as a bridge to connect the microwave frequency and the optical frequency. This finding opens a way for the high-precision optical frequency metrology [3]. But during a long time, the immaturity of the ultrashort pulse laser technology and the highly nonlinear fiber technology at that time limited the development of OFCs. The transition from mode-locked lasers to OFCs faced two problems: Short pulses and frequency locking. The former corresponds to a wider frequency spectrum, and the latter guarantees higher stability. After the Ti:sapphire Kerr-lens femtosecond mode-locked pulse laser [4] was developed in 1991, broadband mode-locked pulses became feasible, but the problem of frequency lock still needed to be solved. In 2000, Jones et al. [5] realized the carrier-envelope phase of femtosecond mode-locked lasers controllable with a heterodyne system, obtaining full stabilized OFC, which is applicable for absolute optical frequency measurement with unprecedented performance. With the increasing development of fiber mode-locked lasers, OFCs based on fiber mode-locked lasers developed rapidly. In 2006, Swann et al. [6] developed the fiber-laser frequency comb with its relative linewidth <1 Hz. It suggested that the frequency stability and phase noise characteristics of OFC based on fiber mode-locked lasers could meet a variety of measurement needs [7-9].

* Corresponding author.

** Corresponding author.

E-mail addresses: 202021010138@std.uestc.edu.cn (H. Zhang), 202111012142@std.uestc.edu.cn (B. Chang), 202121010139@std.uestc.edu.cn (Z. Li), 2018190607032@std.uestc.edu.cn (Y.-P. Liang), qinchenyue_1997@std.uestc.edu.cn (C.-Y. Qin), 202022010139@std.uestc.edu.cn (C. Wang), hdxia2008@sina.com (H.-D. Xia), tanteng_ph.d@std.uestc.edu.cn (T. Tan), yaobaicheng@uestc.edu.cn (B.-C. Yao).

¹ Authors contributing equally.

<https://doi.org/10.1016/j.jnest.2022.100157>

Received 14 October 2021; Received in revised form 26 April 2022; Accepted 28 April 2022

Available online 12 May 2022

1674-862X/© 2022 University of Electronic Science and Technology of China. Publishing Services provided by Elsevier B.V. on behalf of KeAi Communications Co. Ltd. This is an open access article under the CC BY-NC-ND license (<http://creativecommons.org/licenses/by-nc-nd/4.0/>).

Microcavity Kerr OFC is a new type of OFCs birthing in the 21st century, which is produced based on the four-wave mixing (FWM) effect in the high quality factor (Q) optical microcavity [10]. Thanks to the highly compact geometry, the comb tooth spacing could be in the range from tens of GHz to THz, further expanding the application range of traditional mode-locked laser combs. Based on the integrated microcombs, more applications, such as precision frequency calibration [11], arbitrary waveform generation [12], astronomical spectrum calibration [13], soliton transmission [14], the optical communications technology [15], and optical storage [16], have been reported. The development of Kerr OFC is closely related to the progress of the microcavity manufacturing process. In 2003, Armani et al. [17] demonstrated a process for producing silica toroid-shaped microresonators on a chip with Q in excess of 100 million. Then in 2004, they reported Kerr-nonlinearity induced optical parametric oscillation (OPO) in a microcavity for the first time [18]. In 2007, Del'Haye et al. [19] utilized continuous-wave pumping and realized broadband Kerr OFC in a microdisk cavity, which opened a new chapter in the study of Kerr OFCs. In 2014, Herr et al. [20] systematically investigated temporal dissipative Kerr solitons (DKSs) in a continuous-wave laser-driven nonlinear optical microresonator, which offered a way for solving the problem that the state of modulation instability (MI) lacks high coherence. Since then, the development of microcombs has entered a boom period and derived versatile development directions, forming more and more functions in the field of information science. Fig. 1 shows a brief development roadmap of OFCs [5,6,17–24].

In this review, we will first introduce the principle and theoretical model of OFCs in Section 2. Then we will discuss several types of OFCs in Section 3 and review the applications of OFCs in Section 4. Finally, the future development trend of microcombs and its prospects will be analyzed in Section 5.

2. Principle

2.1. Fundamental principle of OFCs and the self-referencing technology

In principle, OFC appears in the frequency domain as an optical frequency sequence with equal frequency intervals, and in the time domain as an ultrashort optical pulse (an electromagnetic field oscillation envelope with a femtosecond time width) sequence. The spectrum of OFC and its optical pulse sequence satisfy the Fourier transform, as shown in Fig. 2 (a). In the time domain, the relative phase between the carrier (solid) and the envelope (dotted) evolves from pulse to pulse by the amount $\Delta\phi$. In the frequency domain, the elements of the frequency comb of a mode-locked pulse train are spaced by f_{rep} . As mentioned earlier, the generation of OFCs requires frequency locking. In 2000, Jones et al. proposed the f - $2f$ self-reference frequency locking method to measure the absolute frequency of a mode-locked laser [5]. Mode-locked lasers generate periodic laser pulse trains. The periodic laser pulse sequence in the time domain is converted into the frequency space, and it can be expressed as a spectrum containing equally spaced frequencies. The overall intensity of the spectrum is adjusted by the envelope of the laser pulse. Therefore, it is similar to an optical ruler in the frequency domain, and the minimum scale is equal to the repetition frequency of the mode-locked laser.

The frequency of each comb line of OFC can be expressed as

$$f_n = f_{\text{CEO}} + n f_{\text{rep}} \quad (1)$$

where f_{CEO} is the carrier envelope offset frequency, f_{rep} is the repetition frequency of the optical pulse, and n is the order of OFC. In large-number studies, there are three types of frequency combs: Incoherent combs where neither f_{CEO} nor f_{rep} is stabilized, coherent combs where only f_{rep} is locked, and fully-stabilized combs where both f_{rep} and f_{CEO} are locked with one frequency reference [5].

When the spectral width of OFC reaches one octave, the n th order comb is frequency-multiplied, and the frequency of the new light wave after frequency multiplication can be expressed as

$$2f_n = 2f_{\text{CEO}} + 2n f_{\text{rep}}. \quad (2)$$

The $2n$ th order comb line frequency is

$$f_{2n} = f_{\text{CEO}} + 2n f_{\text{rep}}. \quad (3)$$

The cavity length of the laser is controlled through the feedback network, thereby locking the carrier envelope offset frequency f_{CEO} , that is, the locking of the carrier envelope phase is realized. At the same time, the feedback network is used to lock the repetition

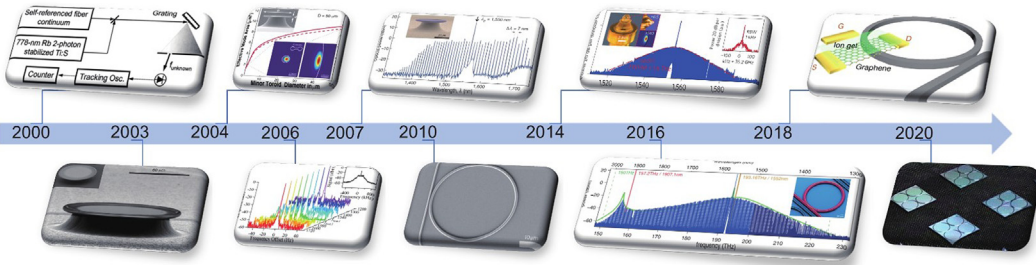


Fig. 1. Main development path of OFCs [5,6,17–24].

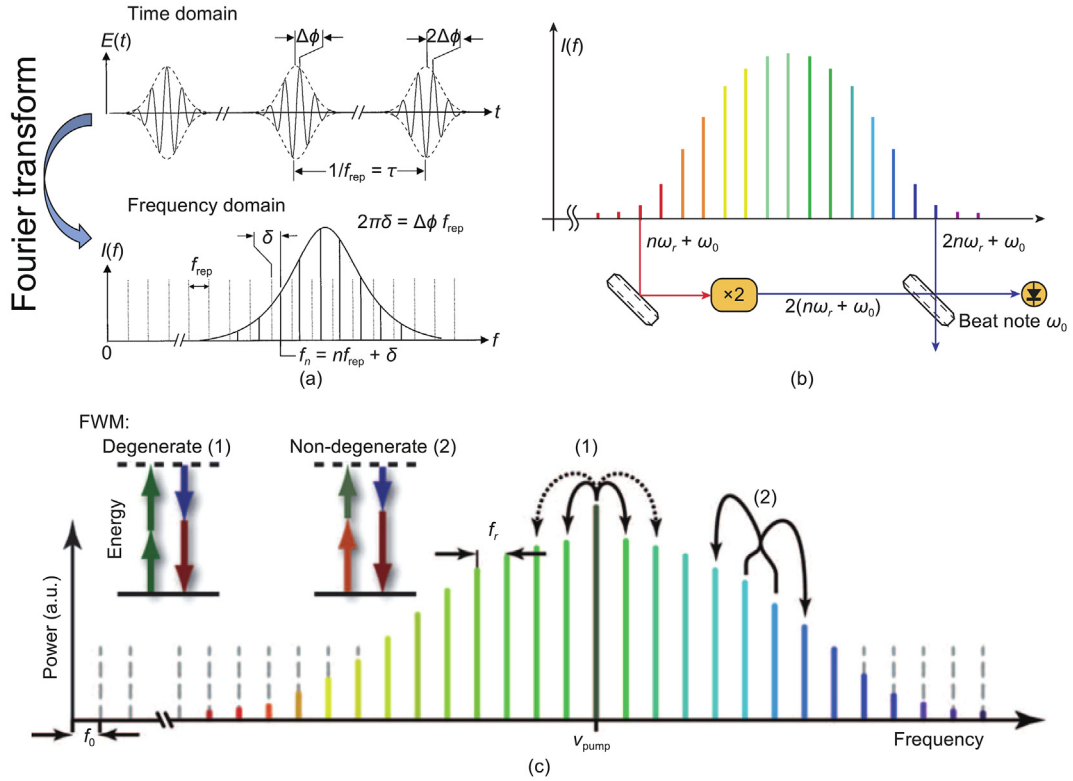


Fig. 2. OFC generation mechanism: (a) time-domain and frequency-domain images of OFC [5], (b) f - $2f$ self-reference frequency locking principle [3], and (c) generation of OFC by the FWM effect [25].

frequency f_{rep} of the laser, so as to realize the frequency lock of each comb line of OFC. Typical f - $2f$ self-reference frequency-locked OFC is shown in Fig. 2 (b).

2.2. FWM effect for OFCs generation

When light travels in a nonlinear medium and the energy reaches the threshold, the nonlinear effects of the medium (such as cross-phase modulation (XPM), self-phase modulation (SPM), and FWM) can be excited. FWM is the main nonlinear effect that produces microcavity Kerr OFC. In the FWM process, the two photons with frequencies of ω_1 and ω_2 annihilate, and two new photons with frequencies of ω_3 and ω_4 are generated at the same time. The energy conservation is satisfied during the parametric process:

$$\omega_1 + \omega_2 = \omega_3 + \omega_4. \quad (4)$$

In some cases when $\omega_1 \neq \omega_2$, it is also called non-degenerate FWM. In the case of degenerate FWM, only one beam of pump light is needed to realize the FWM process. When the appropriate dispersion conditions (usually anomalous dispersion) are met, it will generate an efficient FWM effect between the longitudinal modes in the microcavity. Utilizing single-frequency continuous light to pump the microcavity, the primary sideband can be formed by degenerate FWM when the pump power exceeds a certain threshold. The primary sideband and the pump light further realize the broadening of the spectrum by cascading FWM to form OFC [25]. The process of FWM to generate OFC is shown in Fig. 2 (c).

2.3. Brief theoretical model of OFCs

In order to deeply understand the physical mechanism of OFCs, here we briefly introduce the theoretical model of OFC. In 2010, Chembo and Yu [26] derived the dynamic equation describing the transmission of light in the whispering gallery mode (WGM) microcavity based on the Maxwell wave equation, that is, the nonlinear coupled mode equation:

$$\dot{\mathcal{A}}_\eta = -\frac{1}{2} \Delta\omega_\eta \mathcal{A}_\eta - i g_0 \sum_{\alpha, \beta, \mu} \Lambda_\eta^{\alpha, \beta, \mu} \mathcal{A}_\alpha \mathcal{A}_\beta^* \mathcal{A}_\mu e^{i\varpi_{\alpha, \beta, \mu, \eta} t} + \frac{1}{2} \Delta\omega_\eta \mathcal{T}_\eta e^{i(\Omega_0 - \omega_\eta)t} \quad (5)$$

where \mathcal{A}_η is the normalized electric field of mode η , $\Delta\omega_\eta$ is the modal bandwidth, g_0 is the FWM gain, α , β , μ , and η are the four interacting modes in the microcavity, $\Lambda_\eta^{\alpha,\beta,\mu}$ is the inter-mode coupling coefficient, $\varpi_{\alpha,\beta,\mu,\eta}$ is the FWM frequency detuning, \mathcal{F}_η is the external cavity pump, Ω_0 is the pump frequency, ω_η is the resonance frequency of the η -order mode, and t is the time.

The basic idea of this method is to establish a set of rate equations in the time domain, and use the equations to study the effects of the nonlinearity, dispersion, absorption, and coupling losses of the optical microcavity on the mode transmission process. The research results show that the dispersion characteristics of the microcavity play an important role in the generation of the comb spectrum. In the negative dispersion region, the MI process is a significant physical mechanism for the generation of comb spectra. The nonlinear coupled mode equation can describe the evolution process of microcavity OFC, but it is difficult to calculate the case with a large number of modes.

In 2013, Coen et al. [27] used the Lugiato-Lefever equation (LLE), to describe the evolution of the optical field in the optical microcavity and the generation of comb spectra as

$$i \frac{\partial A}{\partial T} = \frac{c\beta_2}{2n_0} \frac{\partial^2 A}{\partial t^2} - g \left| A \right|^2 A - \left(i \frac{\kappa}{2} - \delta\omega \right) A + i \sqrt{\frac{\kappa\eta P_{in}}{\hbar\omega_0}} + g\tau_R A \frac{\partial |A|^2}{\partial t} \quad (6)$$

where A is the temporal envelope of the intracavity pulse, T and t represent the fast and slow variables of time, respectively, ω_0 is center frequency of the cavity mode, $g = \hbar\omega_0^2 n_2 D_1 / 2\pi n_0 A_{eff}$ is the Kerr nonlinear gain coefficient, $\kappa = \omega_0/Q$ is the power dissipation rate corresponding to the soliton mode, P_{in} is the pump power, c is the speed of light, n_0 is refractive index of the microcavity, n_2 is the nonlinear coefficient of the microcavity, β_2 is the second-order dispersion coefficient of the microcavity, $D_1/2\pi$ is the free spectral range (FSR) of the microcavity, $\eta = Q/Q_E$ is the coupling coefficient, Q is the total quality factor, Q_E is the coupling quality factor, A_{eff} is the effective mode area of the waveguide, and τ_R indicates the Raman shock time. The last item of (6) indicates the material Raman contribution to the soliton self-frequency shift [28], resulting that the center frequency of the spectrum is spectrally red-shifted from the continuous-wave pump laser. Nowadays LLE is widely used in the theoretical study of the generation of microcavity Kerr OFCs, including various domains and dynamics of OFCs. By solving the steady-state solution of the equation, it is found that the generation of the comb-shaped spectrum and the formation of the time-domain soliton pulses have a certain connection with the radiation of dispersive waves [29]. By scanning the detuning of the pump light, LLE can be used to obtain the evolution process of the light field in the cavity, including the main comb state, the sub-comb, the MI comb, the breathing soliton comb, and the stable soliton frequency comb. At the same time, other nonlinear physical processes in the microcavity can also be simulated and predicted by LLE, such as Raman self-frequency shift, dispersive wave, and XPM.

3. Types of OFCs

3.1. OFCs based on mode-locked lasers

The development of broadband OFCs is closely related to femtosecond mode-locked lasers, with the increasing maturity of fiber mode-locked lasers, OFCs based on fiber mode-locked lasers have developed rapidly. In 2006, Swann et al. [6] realized a mode-locked laser frequency comb with the comb linewidth less than 1 Hz, and they experimentally verified that the erbium-doped fiber mode-locked laser OFC has characteristics comparable with Ti:sapphire frequency combs in terms of phase noise and frequency stability [5,6]. The frequency stability and phase noise characteristics of OFC based on fiber mode-locked lasers can meet the needs of a variety of measurement through rigorous design. Besides, OFCs based on fiber mode-locked lasers have huge advantages for current and future applications in terms of the repetition frequency, spectral flatness, robustness, size, and spectral range [6,8]. In 2012, Ycas et al. [30] reported a multibranch laser frequency comb based upon a 250-MHz mode-locked erbium-doped fiber laser that spans more than 300 THz of the bandwidth, from 660 nm to 2100 nm, which expanded the application of laser frequency combs in the near-infrared field. In the same year, Cingöz et al. [31] reported an extreme ultraviolet frequency comb with a wavelength of 40 nm by coupling a high-power near-infrared frequency comb and a robust femtosecond enhancement cavity together. The extreme ultraviolet frequency comb is promising to extend ultra-high-precision spectroscopy to the spectral region below 100 nm. In 2021, Lesko et al. [32] reported a scalable source of near-single-cycle pulses from a robust and low-noise erbium fiber mode-locked laser, obtained a comb spanning six octaves, from the ultraviolet to the mid-infrared (mid-IR). In addition, researchers are still actively carrying out research on fiber frequency combs, such as multi-branch OFCs [31,33], OFCs with different wavelengths [34], OFC systems with an adjustable repetition frequency [35,36], and arbitrary optical frequency synthesis systems [37,38]. OFCs based on mode-locked lasers are developed rapidly and explored widely, but the bulky size, relatively high cost, and complex control, to some extent, limit their engineering applicability.

3.2. OFCs based on microcavities

Based on the early research on the microcavity conducted by Vahala et al. [17,18], Del'Haye et al. [19] realized broadband Kerr OFC in a microtoroid cavity in 2007, they used a continuous-wave laser with the power of 130 mW and the center wavelength of 1555 nm to pump a silicon microtoroid cavity with a diameter of 75 μm , and then obtained high-repetition OFC with a spectral width of 500 nm, as shown in Fig. 3 (a). Since then, many studies on the frequency comb of the microcavity have emerged. In 2008, Savchenkov et al. [39] reported a tunable monolithic OFC generator based on a crystalline calcium fluoride WGM resonator. By tuning the frequency of the pumping laser with respect to the corresponding resonator mode, they could select a deterministic integer number of FSR of the

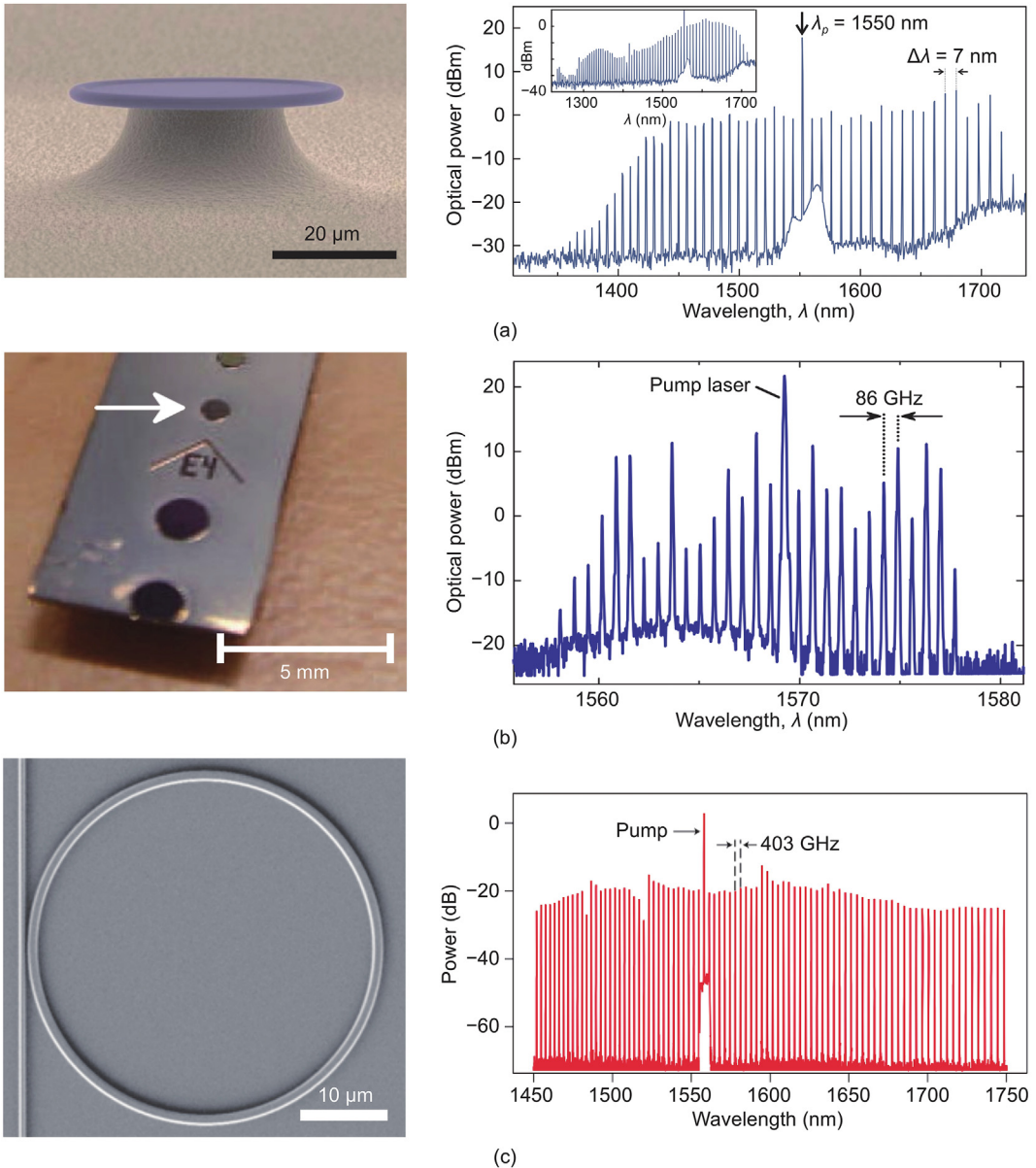


Fig. 3. Generation of typical OFCs: (a) image of a toroid microcavity on a silicon chip and OFC generated from the microcavity [19], (b) image of a silicon chip with a row of 750- μm -diameter monolithic toroidal microresonators and spectrum of OFC, generated by pumping one of the microresonators [40], (c) image of a silicon nitride microring resonator coupled to a bus waveguide and pump output spectrum of the microresonator [21].

resonator, that is, tuning the frequency spacing of the comb. In the same year, Del'Haye et al. [40] reported OFC generated by FWM in a monolithic microresonator whose mode spacing is in the microwave regime (86 GHz), as shown in Fig. 3 (b). They demonstrated that it was possible to control the two degrees of freedom of the microcavity frequency comb (MFC) spectrum, which is required for full stabilization of the comb spectrum.

In 2010, Levy et al. [21] successfully prepared a microring resonator with a Q factor of 5×10^5 by using the silicon nitride waveguide with a cross section of $1700 \text{ nm} \times 711 \text{ nm}$, and experimentally observed OPO in the integrated microring resonator, resulting in a Kerr comb with a spectral range of 300 nm and FSR of 403 GHz. Images and experimental results of the integrated microresonator are shown in Fig. 3 (c). In the same year, Chembo and Yu [26] reported OFC generated with a monolithic WGM resonator. It is vital that they have proved that the interaction between the dispersion and Kerr nonlinearity affects the spectrum of the generated comb. In particular, they have shown that the pump first excites a primary comb through degenerate FWM, and then cascades out secondary combs through non-degenerate FWM. They have done numerical simulation for this, and the results showed that the theory was in good agreement with the experiment.

Early microcavity OFCs often operate in the MI state without locking, thus they cannot form a stabilized ultrashort pulse train [41–43]. The emergence of DKS solves these problems [44]. The formation of DKS stems from the double balance between the dispersion and nonlinearity as well as the loss and parametric gain. In 2014, Herr et al. [20] reported DKS in a continuous-wave laser-driven nonlinear optical microresonator for the first time. Fig. 4 (a) shows the experimental design and part of the results. This experiment became a landmark in the development of Kerr OFCs, and the subsequent research mainly focused on generating soliton frequency combs and related applications. In the next year, Yi et al. [42] demonstrated soliton mode locking in high-Q silica resonators, and they also gave a method for the long-term stabilization of the solitons, which was also used to test the theoretical dependence of the comb power, efficiency, and soliton existence power on the pulse width. Fig. 4 (b) shows the experimental setup and a soliton state with this

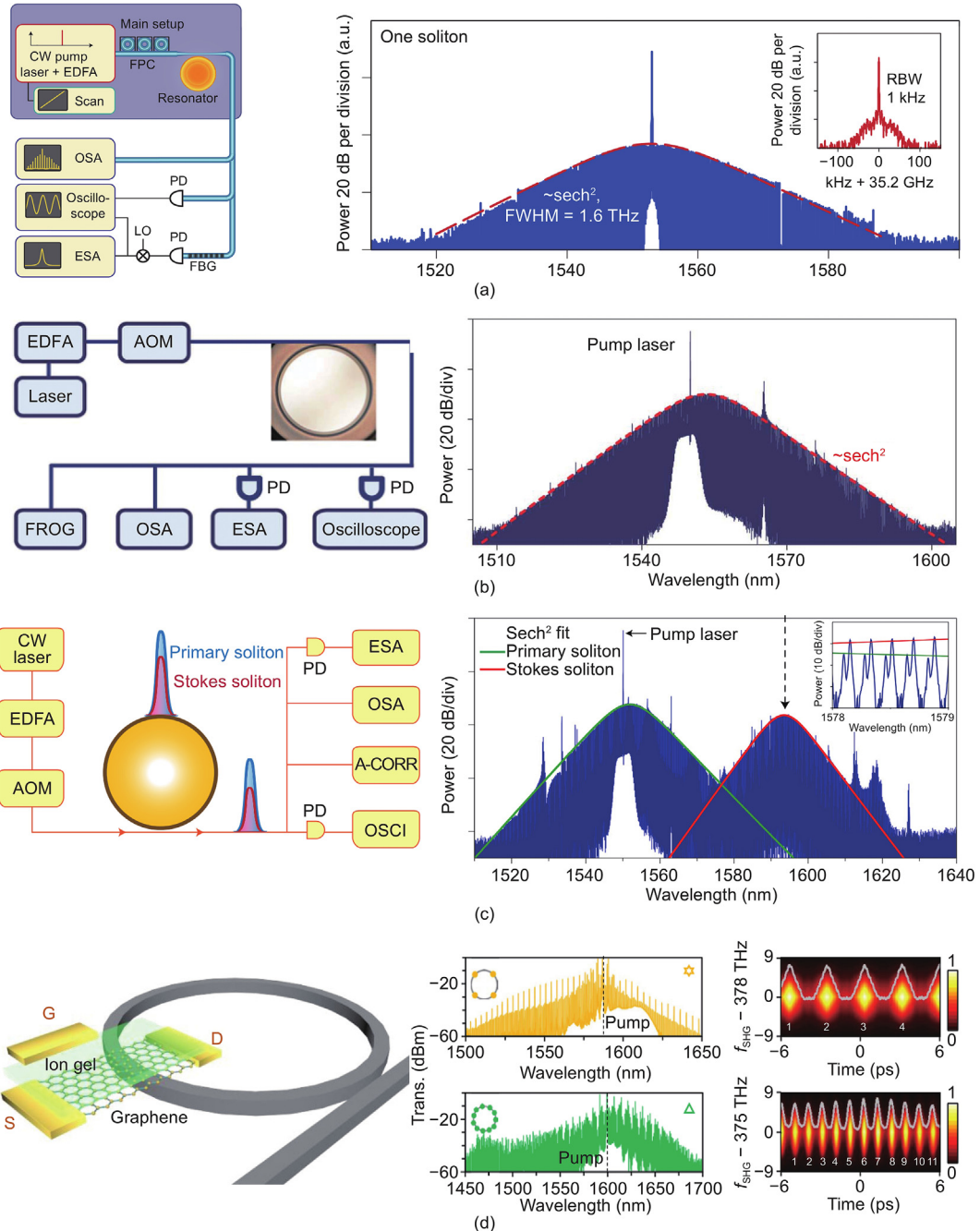


Fig. 4. Generation and tuning of an optical soliton frequency comb: (a) OFC generation device and soliton spectrum [20], (b) soliton comb generation experimental setup and a single soliton spectrum [42], (c) experimental setup and description of Stokes soliton generation [46], and (d) gate-tunable graphene-nitride heterogeneous microcavity and periodic soliton crystal states tuning [23].

method. Later in 2016, they used an active feedback method to both capture specific soliton states and stabilize the states indefinitely. The capture and stabilization method is simple to implement, relying on servo control of the pump laser frequency by measuring the soliton average power [43]. And this technique provides a practical route for stable soliton excitation in any application of soliton mode locking, including frequency combs. In the same year, Brasch et al. [45] reported a method named “power kicking” to overcome the instability caused by the change of cavity power by modulating the power of the pump laser. And once a stable soliton state is generated inside the microresonator, it can exist for hours and potentially much longer if the perturbations from outside (mostly drifts in the pump power and pump laser frequency) are not too large. And the Stokes soliton in optical microcavities was also reported in the same year. Yang et al. [46] reported the Stokes soliton, which was not previously observed in optical systems. The experimental setup and results are shown in Fig. 4 (c). The Stokes soliton forms and regenerates by optimizing its Raman interaction in space and time within an optical potential well shared with another soliton. The Stokes soliton is the second type of solitons to be observed in microcavities (beyond DKSS [20]) and also represents that soliton trapping can be observed in any microcavities. A recent study shows the unique potential of the Stokes soliton in the field of sensing [47]. With the continuous progress of dispersion engineering, the observation and control of the position of the Stokes soliton in the spectrum will be feasible. So far, in order to achieve stable soliton generation [48], a series of schemes have been proposed to keep the system in equilibrium when the pump light is in a red detuning state [49], which includes the frequency tuning [20], auxiliary laser [50], thermal tuning [51], photorefractive effect [52], self-injection locking [53], piezoelectric control [54], and pulse pump [55].

The emergence of solitons has greatly promoted the development of OFCs. In order to further promote the development of OFCs, researchers tried to tune OFCs [56]. For example, in 2018, Yao et al. [23] reported the gated intracavity tunability of graphene-based OFCs, by coupling the gate-tunable optical conductivity to a silicon nitride photonic microresonator, thus modulating its second- and higher-order chromatic dispersion by altering the Fermi level. As shown in Fig. 4 (d), a graphene/ion-gel heterostructure is incorporated in the nitride microresonator with the advanced integration technology, and it can be used to tune the properties of the microresonator. The realization of this graphene heterostructure provides a new way of the controllable frequency comb and soliton dynamics. In 2020, Liu et al. [54] monolithically integrated aluminum nitride actuators on ultralow-loss silicon nitride waveguides and successfully realized the piezoelectric control of a soliton microcomb (SMC). This work endowed SMCs with integration, ultralow power, and fast actuation, expanding the application range of microcombs. In the same year, Tan et al. [57] realized the chiral soliton in a packaged microresonator. This soliton OFC had good performance with an agile on-off switch and tunable dual-comb generation, which brought fast tunable soliton tools within reach. In the next year, Lu et al. [58] introduced the external control light field, and realized the trapping and manipulation of the soliton through the intracavity optical field potential well formed by the beat frequency of the pump light, and obtained synthetic soliton crystal OFC with the solitons arranged at equal intervals in the cavity. Furthermore, the ordered temporal distribution also coherently improved the power of comb lines. That means, the total power of the N -solitons crystal optical comb was increased by N times compared with the single soliton, and the single comb lines power was increased by N^2 times, which paved the way to the application of high-power microcavity OFCs and effective manipulation of cavity solitons.

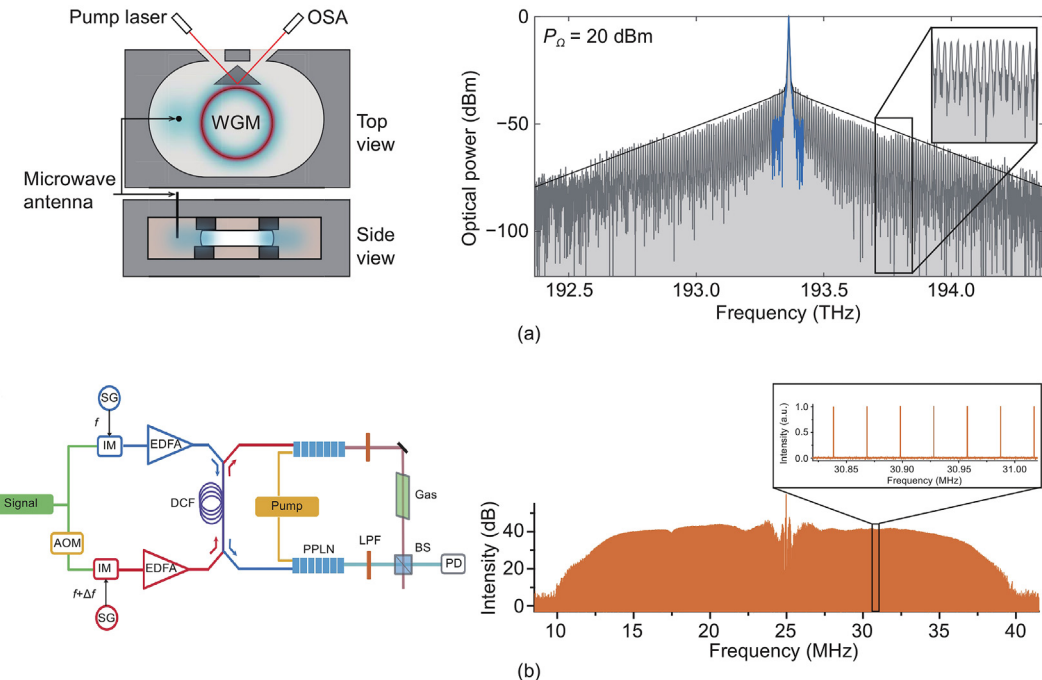


Fig. 5. EO frequency combs: (a) setup and spectrum of the EO frequency comb based on WGM resonators [59] and (b) experimental setup and spectrum of the EO comb [62].

3.3. Electro-optic (EO) frequency combs

OFCs based on the EO modulation technology can exactly meet these needs of flexible adjustability, which have attracted growing interest in recent years. In 2019, Rueda et al. [59] reported a broadband frequency comb realized through the EO effect within a high-Q WGM resonator. Fig. 5 (a) shows the setup and spectrum of the EO comb. Such a device was fully integrated and could operate at low microwave and optical power. Different from common third-order Kerr nonlinear OFC, this frequency comb relies on the second-order nonlinear effect and is more efficient. In the same year, Zhang et al. [60] realized an integrated EO comb generator with a large EO response and ultralow optical loss in a thin-film lithium niobate photonic platform, which was almost two orders of magnitude larger than prior integrated EO combs. This work suggests that dispersion engineering and high-frequency modulation had great potential in octave-spanning EO comb generators.

Besides, there are EO combs that rely only on modulators, not the cavity. In 2007, Sakamoto et al. [61] reported an EO comb with a conventional Mach-Zehnder modulator and demonstrated 10-GHz spaced ultraflat OFC generating a 10-dB bandwidth of 230 GHz. In 2017, Yan et al. [62] reported a difference frequency generation method which uses an EO modulator to generate frequency-agile near-infrared frequency combs, as shown in Fig. 5 (b). This work extended the operation of dual-comb spectroscopy (DCS) with EO modulators to the mid-IR range. Compared with traditional OFCs, one of the advantages of EO combs is that they originate from continuous-wave lasers with a tunable frequency. In this way, the comb produced by the EO device is also frequency-tunable, since the EO modulator usually has a larger working frequency bandwidth. Another advantage of EO combs regarding the repetition frequency is their flexibility without modifying the setup [63]. And the convenient connection with standard EO components is also an eye-catching advantage of EO combs.

3.4. Other frequency combs

In addition to OFCs introduced above, there are also other schemes to generate appealing microcomb sources, such as the quantum cascade laser (QCL) based combs and oscillators based on $\chi^{(2)}$ platforms.

QCL is a cascaded structure, and its active area is composed of dozens or even hundreds of repeated cycles, and electrons release photons in each cycle, which greatly increases the output power of the device. OFC produced by QCL has the characteristics of compactness, high precision, high stability, and high output power [64,65], and can be combined with traditional Fourier spectroscopy as a broadband laser source. QCL-based OFCs currently show the lowest size, weight, and power consumption because they are electrically pumped. In 2012, Hugi et al. [66] presented mid-IR QCL free-running OFC whose comb linewidth was 1.3 MHz with a narrow intermode beat linewidth of 200 Hz. Importantly, the carrier-envelope offset frequency and the repetition frequency can be independently tuned by changing the direct current and radio-frequency injection, opening the way to metrological and sensing applications. In 2019, Consolino et al. [67] reported the full-phase-stabilization of a QCL comb against the primary frequency standard, proving independent and simultaneous control of the two comb degrees of freedom (the modes spacing and the frequency offset) at a metrological level. The results show that QCL combs are well suited for the most demanding applications, achieving the Hz-level stabilization of each individual emitted mode, and it can be applied to dispersion-compensated devices to ensure broader spectral coverage at higher operating currents.

In recent years, all-fiber microcavity OFCs have made new progress in order to meet the demand for direct access to optical fiber systems. It has several unique advantages: Multiple gains, flexible material control, a high Q factor, a simple structure, convenient processing, and low cost. And more importantly, it is especially suitable for mass production. In 2020, Jia et al. [68] reported a compact photonic flywheel with a sub-femtosecond time jitter (the average time up to 10 μ s) at the quantum-noise limit of a monolithic fiber resonator. In this work, the researchers used a stimulated Brillouin laser in a fiber microcavity to indirectly pump a fiber microcavity to attain OFC. The noise of OFC can break through the noise limit of the pumped laser and generate a stable thermal soliton, which approaches the lower quantum noise limit of the fiber microcavity. In the same year, Qin et al. [69] reported an electrically controllable laser frequency comb in graphene-fiber microresonators, which utilized graphene optoelectronic feedback to complete the repetition frequency, pulse control, and active feedback stabilization, and realized a laser frequency comb with an all-fiber output. Such a device is expected to achieve mass production with the success of the industrialized production of graphene optical fibers [70].

4. Applications

4.1. Optical communications

With the advent of the era of big data interconnection, the demand of the communications bandwidth has greatly increased because of the growth of modern information networks. Developing terabit coherent optical communications systems becomes an effective way to solve this problem. Laser sources with a narrow linewidth and high optical signal-to-noise ratio (OSNR) are strongly needed in coherent optical communications [71]. OFC features a high repetition frequency, low noise, narrow linewidth, high-frequency stability, and wide spectrum which means the spectral range can reach several hundred nanometers, covering multiple communications bands, including C-band and L-band, thus it could be very attractive as multi-carrier sources in wavelength-division multiplexing (WDM).

A typical WDM coherent communications system is shown in Fig. 6 (a) [72], in the transmitter section, single OFC with multiple lines (on which the optical carriers encode data) is used as the light source which can replace hundreds of tunable continuous-wave lasers. The comb lines are separated by the de-multiplexer (DEMUX). For modulators, each channel is equivalent to a single continuous-wave source. Next, the amplitude and phase of each optical carrier are modulated in the in-phase/quadrature modulator (IQ-mod) to carry

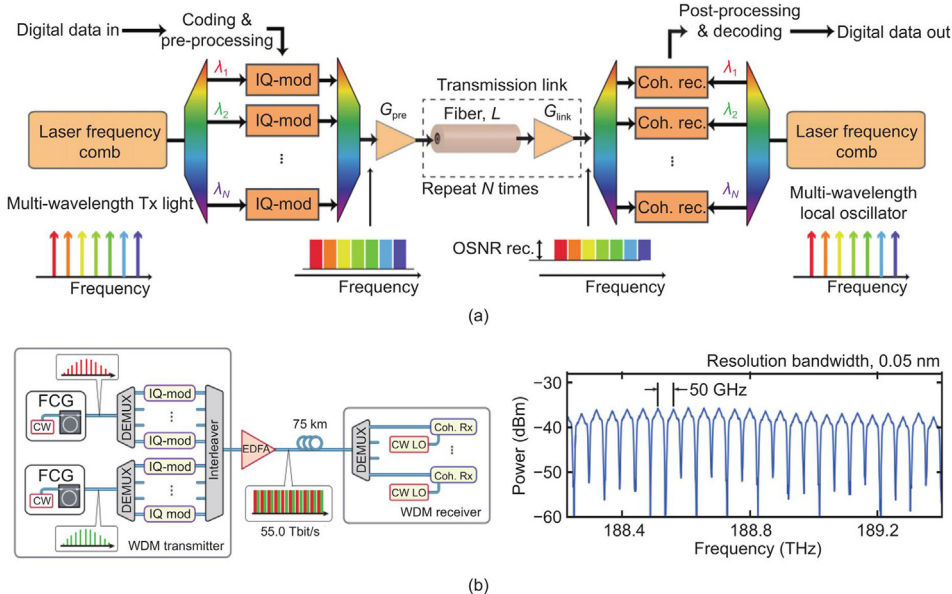


Fig. 6. OFC for communications: (a) schematic of a WDM coherent communications system [72] and (b) principle of communications using a pair of interleaved DKS combs at the transmitter (left) and optical spectrum of the WDM data stream (right) [76].

information. Then, all the data channels are integrated into one channel by the multiplexer (MUX) and amplified by an erbium-doped fiber amplifier (EDFA) before long-distance transmission. The same principle is applied to the receiver. There are three main advantages of this system. First, comb-based superchannels make the WDM channels to be more densely packed [73], which greatly improves the volume and rate of information transfer. Second, the stable spacing and broadband phase coherence of comb lines enable high spectral efficiency transmission and allow for a pre-compensation of fiber nonlinearity [74]. Third, joint digital signal processing is supported to reduce complexity or increase phase-noise tolerance [73].

In 2015, Temprana et al. [75] predicted and solved the problem of signal distortion in optical fiber transmission by using a parametric frequency comb derived from a single continuous-wave master oscillator. Without the use of relay amplifiers, the effective transmission distance could exceed 12000 km, which could directly transmit 20-times stronger signals than usual. In 2017, Marin-Palomo et al. [76] realized a communications rate of 55 Tbps over a 75-km transmission distance by using low-noise soliton OFC with multiplexing 179 channels, and the corresponding spectral efficiency was increased to 5.2 bit/s/Hz (see Fig. 6 (b)), which greatly improved the quality of data transmission. More importantly, the experiment proved the potential of chip-scale DKS frequency combs for massively parallel WDM at data rates of tens of terabits per second, which means it has great application value in fully integrated communications systems in the future. In the next year, Fülop et al. [77] combined soliton OFC with the traditional superchannel method which achieved high spectral efficiency, reaching 10 bit/s/Hz. And the conversion efficiency of the comb enabled transmitted OSNR above 33 dB. In the same year, Geng et al. [14] utilized a DKS frequency comb generated in an on-chip microcavity to realize seamless channel multiplexing and high bitrate superchannel transmission of coherent optical orthogonal frequency division multiplexing (CO-OFDM) data signals. With a frequency comb bandwidth of 2.295 THz, they achieved the communications rate of 6.885 Tbps.

In general, the OFC based WDM system is a research hotspot in recent years [78,79]. There are two prospective future research areas related to joint processing in comb-based systems [73]. One is to solve the problem of phase noise caused by fiber nonlinearity and the walk-off between the sub-channels caused by dispersion in optical fiber transmission to achieve long-distance transmission [80]. Another is to co-integrate the receiver and transmitter on a chip-level module.

4.2. Photonic microwave generation

For the transmission of the microwave signal, the characteristics of low loss and high bandwidth of the optical fiber system can be used. The high capacity optical fiber information system must involve the high-frequency, large-bandwidth microwave technology. Therefore, the close combination between them gradually formed a new discipline—microwave photonics. At present, microwave photonics has many research directions in devices and systems. Among them, the special role of the OFC technology in signal transformation has attracted increasing attention in recent years.

In 2008, Song et al. [81] reported a monochromatic sub-terahertz signal generation technique using OFC generated from an EO modulator with a continuous-wave laser. This work achieved random or continuous frequency tuning in the range between 100 GHz and up to 1 THz. Especially, for the 125-GHz microwave signal, the phase noise was approximate $-92 \text{ dBc/Hz@10 kHz}$. In 2015, Liang et al. [82] first carried out a microwave signal generation experiment by using microcavity OFC. They utilized a high-speed photodetector to

detect the beat frequency of the OFC line and successfully obtained a high-quality microwave signal. Fig. 7 (a) shows the microcavity image, experimental setup, and phase noise level at 10 GHz. For the 10-GHz microwave signal, its phase noise was better than -60 dBc/Hz@10 Hz, -90 dBc/Hz@100 Hz, and -170 dBc/Hz@10 MHz. In 2020, Lucas et al. [83] realized a microresonator-based Kerr frequency comb with a 14-GHz repetition rate generated from an ultra-stable pump laser and then used it to derive an ultralow-noise microwave reference signal, whose absolute phase noise level is below -60 dBc/Hz@1 Hz and -135 dBc/Hz@10 kHz. In August of the same year, Liu et al. [84] generated the microwave signal in the X-band and K-band by using integrated SMC. This work used a silicon nitride microring cavity prepared by the complementary metal-oxide-semiconductor (CMOS) transistor compatible process with the Q factor of 2.3×10^7 , and thus the microwave signal phase noise is not very good compared with the results of previous work, as shown in Fig. 7 (b). However, the advantage of this scheme is that it can achieve on-chip integration, and it presents great potential to reduce the phase noise by using lasers with suppressed phase noise and relative intensity noise (RIN). Taking advantage of microresonators with a higher Q factor is an optional way, which depends on the progress of the CMOS technology. In 2021, Bai et al. [85] offered another scheme to generate microwave signals with low phase noise. First, they used the pump light to generate a Brillouin laser, and then the Brillouin laser was used to excite Kerr OFC as a new pump light source. Utilizing the advantages of the stable frequency and narrow linewidth of the Brillouin laser greatly reduces the phase noise of microwave signals. Fig. 7 (c) shows the generation principles and phase noise of the 10-GHz microwave signals, which is -49 dBc/Hz@10 Hz, -130 dBc/Hz@10 kHz, and -158 dBc/Hz@20 MHz, respectively.

In addition to the typical representative work introduced above, there are still many excellent studies reported recently, such as the photonic radio-frequency (RF) arbitrary waveform generator [86] and photonic RF and microwave integrator/differentiator [87], which show the broad application prospects of OFCs in the field of microwave photonics.

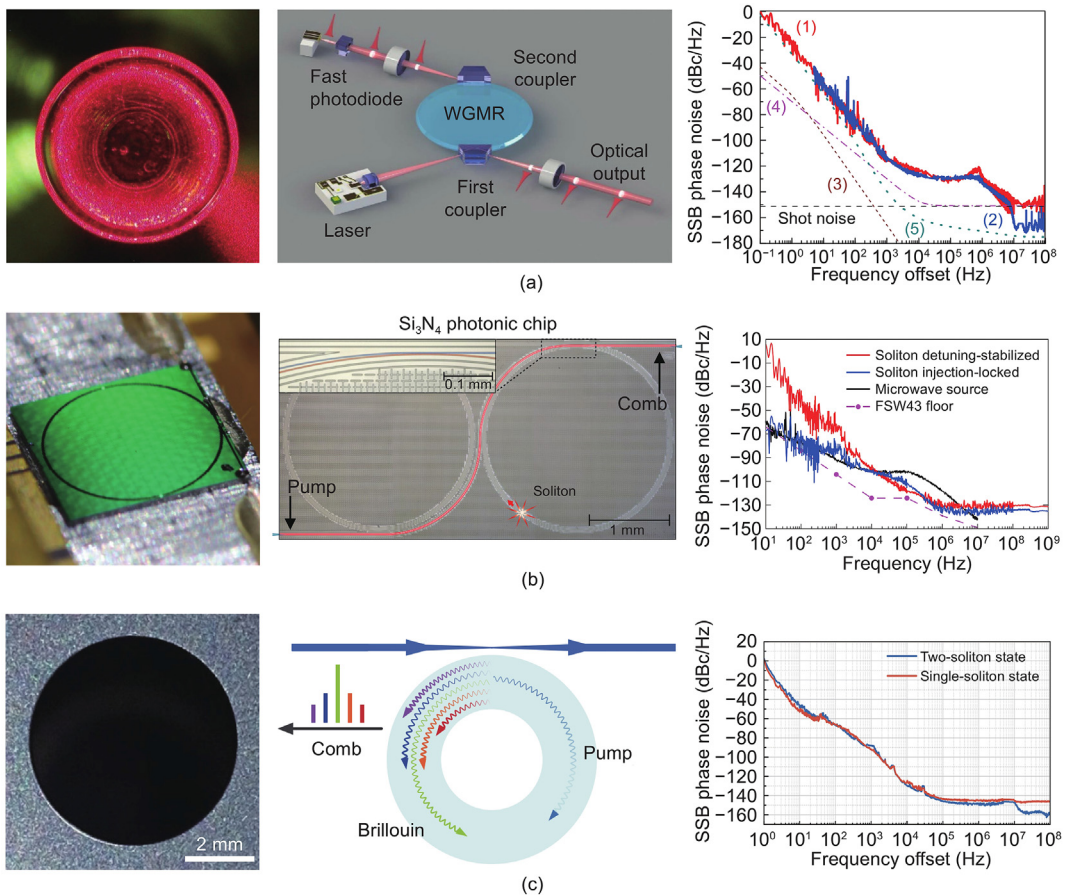


Fig. 7. Low phase noise microwave signals produced by OFCs: (a) diagram of the setup with a WGM microcavity and phase noise of the 10-GHz RF signal [82], (b) principle of photonic microwave generation through a silicon nitride chip and phase noise characterization of the soliton repetition rate [84], and (c) photograph of the disk resonator, diagram of the Brillouin-Kerr soliton frequency comb, and phase noise of the soliton repetition rate [85].

4.3. Ranging

The application of OFCs in light detection and ranging (LIDAR) was first demonstrated in 2000 and enables a number of advantages compared with traditional sources [88]. During the last decades, to realize a ranging system with high-precision, long-distance, and high real-time performance, many techniques based on OFCs have been developed which will be introduced below [89], such as the frequency-modulated continuous-wave (FMCW) method [90,91], synthetic wavelength interferometry (SWI) [92–94], dispersive interferometry (DPI) [95–97], time-of-flight (TOF) method [98,99], and dual-comb method [100–102], as well as their combinations [103–105].

FMCW LIDAR uses a coherent ranging method which measures the beat frequency of the local reference light and the echo signal given by an incident laser that is linearly chirped [90]. By the combination of OFC and FMCW, some advantages can be realized. For example, as shown in Fig. 8 (a) [91], the chirp from the pump laser is transferred to all spectral comb teeth of the soliton at once to generate 30 distinct channels, achieving a parallel distance and velocity. Another idea is that a frequency comb can serve as a frequency reference to a continuous-wave laser to reduce the error of frequency modulation (FM) nonlinearity [90].

SWI utilizes different optical modes to generate harmonics of OFC's repetition rate or employs multiple wavelengths referenced to fully stabilized combs (such as multiple-wavelength interferometry (MWI)) [92]. In 2015, Wang et al. [93] demonstrated MWI using four different wavelengths phase-locked to the frequency comb and then determined the absolute distance through a multi-channel scheme of detecting interference phases in parallel. At an update rate of 100 Hz, the linearity error of 1-m travel was less than 61.9 nm. In 2018, the same research group [94] extended a non-ambiguous range for meter-scale measurement by integrating MWI with a direct synthetic wavelength. OFC-based DPI, also known as dispersion interferometry, improves the calculation of the phase-frequency slope of the interference spectrum with a long coherent length and high tolerance against interference [95]. In 2020, Wang et al. [96] reported high-performance LIDAR based on chip-scaled SMC which has an ultrahigh repetition rate that can eliminate the measuring dead zone induced by the mismatch of the repeat frequency of OFC and the resolution of the optical spectrum analyzer. They realized an Allan deviation of 5.6 μm at the average time of 0.2 ms over a long distance of ~ 1179 m with a high speed (up to 35 kHz). Also in 2021, Jiang et al. [97] realized the nanometric precision distance metrology via hybrid spectrally resolved and homodyne interferometry in a single soliton frequency microcomb.

All above methods are based on a single comb. However, they did not make full use of the mode of OFC [95]. Another ranging method that has received widespread attention in recent years is dual-comb ranging (DCR) which solves the distance from the interferograms (IGMs) in time domain or frequency domain by using two OFCs with slightly different repetition rates. As shown in Fig. 8

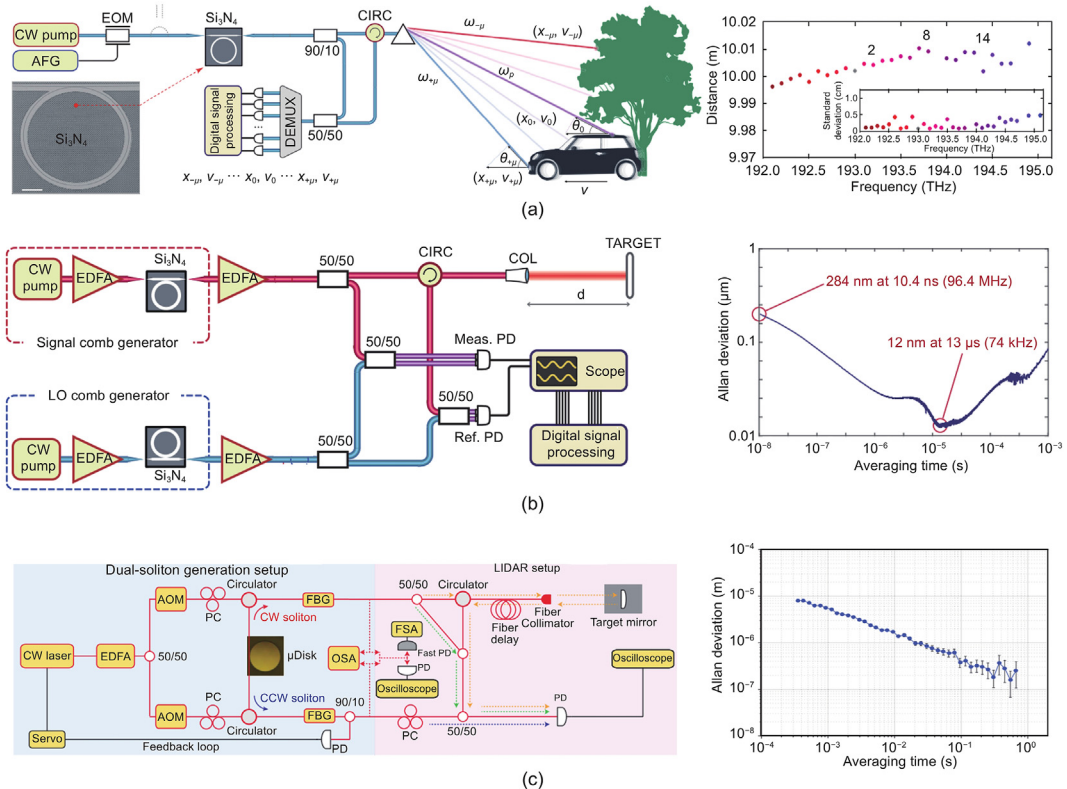


Fig. 8. OFCs for ranging: (a) experimental setup and multichannel distance measurement result of the massively parallel FMCW LIDAR using SMCs [91], (b) experimental setup and Allan deviation of the dual-comb distance ranging system using microresonator soliton frequency combs [100], and (c) experimental setup and Allan deviation of the dual-soliton ranging system using a single pump [101].

(b), Trocha et al. [100] combined the dual-comb method with the TOF method to improve the acquisition speed. By using two soliton Kerr combs generated in the integrated silicon nitride microresonator, they realized ultrafast ranging which allowed for in-flight sampling of the gun projectiles moving at 150 m per second. In 2018, Suh and Vahala [101] reported a simpler system in which a single pump laser was used to generate a dual-frequency comb as counterpropagating solitons in a single microresonator (see Fig. 8 (c)). This system is more compact and integrated. In their research, the 200-nm precision at an average time of 500 ms within a range ambiguity of 16 mm was realized. In 2021, Zhou et al. [102] proposed a dynamic three-degree-of-freedom measurement technique based on dual-comb interferometry and a self-designed grating-corner-cube (GCC) combined sensor which could achieve precise and fast determination of position and direction.

There are three problems need to be solved when using OFC to improve the ranging performance. First, due to the propagation law of pulsed light, there are irreconcilable contradictions in the large measurement range, high resolution, and high measuring speed. Second, as femtosecond pulses usually have a repetition frequency of the order of MHz, the fast photodetector with a wide bandwidth is necessary for detection, which is highly dependent on the performance of the instrument. Third, the ranging system usually has a complex structure and large volume, which substantially restrict the scope of applications. A feasible way to improve system integration is to use microcavity OFCs and on-chip structures of photonic integrated circuits.

4.4. Spectroscopy and sensing

Another popular application field of OFCs is spectroscopy and sensing. While multiple comb-related sensing studies have been reported, such as the sensing system based on the design of a specific cavity structure [106], micro-fiber resonator [107], and fiber nonlinearity (for instance, FWM) [108,109], the most attractive one is DCS [88]. As a non-intrusive absorption spectroscopy technique, the dual-comb asynchronous sampling technology has outstanding advantages, such as the short sampling time, high spectral resolution, and strong multi-component detection ability. It is regarded as a new efficient molecular detection method.

In 2010, Bernhardt et al. [110] built a dual-comb spectrometer generated by two Cr²⁺:ZnSe mode-locked lasers with the wavelength of pulsed light centered at 2.4 μm. This device can achieve 12-GHz resolution within the 10-μs sampling time. The experimental setup and the measured absorption spectrum of C₂H₂ are shown in Fig. 9 (a). The laser spectrum ranges from 1025 nm to 1050 nm. Since the frequencies of the two laser sources of the spectrometer are not locked, the spectrometer is not a light comb in a strict sense. It is only suitable for the spectral analysis with a short sampling time. A long sampling time will have great instability, which seriously affects the accuracy of the spectrum and SNR. In this regard, further improvement is needed. Later, in 2014, the same research group met the demanding stability requirements of the laser combs, and realized real-time DCS. Such a device compensates for the laser instability by electronic signal processing [111]. The principle of adaptive DCS is shown in Fig. 9 (b) as well as the principle of the adaptive sampling spectra.

In 2017, Yang et al. [112] utilized two silica microdisk cavities generated soliton OFC with the repetition frequency of about 22 GHz and the repetition frequency difference of 2.6 MHz. And then they used it to detect the H¹³CN gas absorption peak as shown in Fig. 9 (c). Later in 2019, they realized dual-locked counterpropagating SMCs in a single microcavity, and carried out fine spectral detection with its optical vernier effect. The dual-locked counterpropagating SMCs scheme greatly improved the spectral analysis accuracy [113].

In addition, in 2018, Yu et al. [114] generated dual-OFC covering 2.6 μm–4.1 μm through two independent silicon microring resonators, and measured the absorption spectra of acetone at 2.9 μm–3.1 μm. In 2020, Lin et al. [115] integrated two silicon nitride microring resonators on an optical chip to generate two sets of soliton OFCs with the repetition frequency of about 197 GHz and a difference of less than 10 MHz, and realized the broadband super-resolution detection of the H¹³C¹⁴N gas absorption peak. The detection absorption spectrum width is over 2.3 THz and the scanning resolution is about 319 kHz. In the same year, Wildi et al. [116] reported photo-acoustic dual-frequency comb spectroscopy combined the advantages of photo-acoustic detection and dual-comb's inherent unmatched precision, speed, and wavelength coverage. Fig. 9 (d) shows the experimental setup and the spectrum of the acoustic multi-heterodyne signal for 80-ms and 800-ms long acquisitions. Even though such a device worked in the near-infrared wavelength range, it could be easily transferred to other wavebands only if suitable comb sources were found, which offered chances to fast, sensitive, broadband, and chemically deterministic analysis of gases, liquid, and solids across all wavelengths of light.

Resolution is a significant parameter for spectroscopy. Recently, researchers have developed new methods to improve spectral resolution [117]. In 2021, Bao et al. [118] demonstrated microcomb-based DCS in the mid-IR with GHz resolution, which means 2 orders of magnitude improvement in spectral resolution compared with previous mid-IR microcomb DCS.

4.5. Astrocombs and quantum frequency combs

The high-resolution spectrometer is one of the most important tools in astrophysics, and it plays a key role in searching for Earth-like exoplanets. It also provides new methods for studying dark energy, stability of fundamental constants, and expansion of the universe [119]. Due to its broadband and high-accuracy advantages, OFCs can just meet the needs of astronomical spectrographs. In 2015, Endo et al. [120] reported 15-GHz mode spacing OFC based on a Kerr-lens mode-locked Yb:Y₂O₃ ceramic laser. And this OFC has sufficient long-term stability for the calibration of astronomical spectrographs. In 2019, Suh et al. [121] demonstrated atomic/molecular line-referenced SMC for the calibration of astronomical spectrographs. Fig. 10 (a) shows the experimental concept and optical spectrum of the microcomb. With the chip-scale microcombs, the laser frequency comb systems could be reduced to only a few cubic centimeters, which is an important milestone for future chip-based astrocomb research. In the same year, Obrzud et al. [122] reported a microphotonic astrocomb via temporal DKSS in photonic-chip-based silicon nitride microresonators (see Fig. 10 (b)). The calibration of the astrocomb could reach the precision of 25 cm/s, meanwhile the microphotonic approach enabled broadband astrocombs, free of

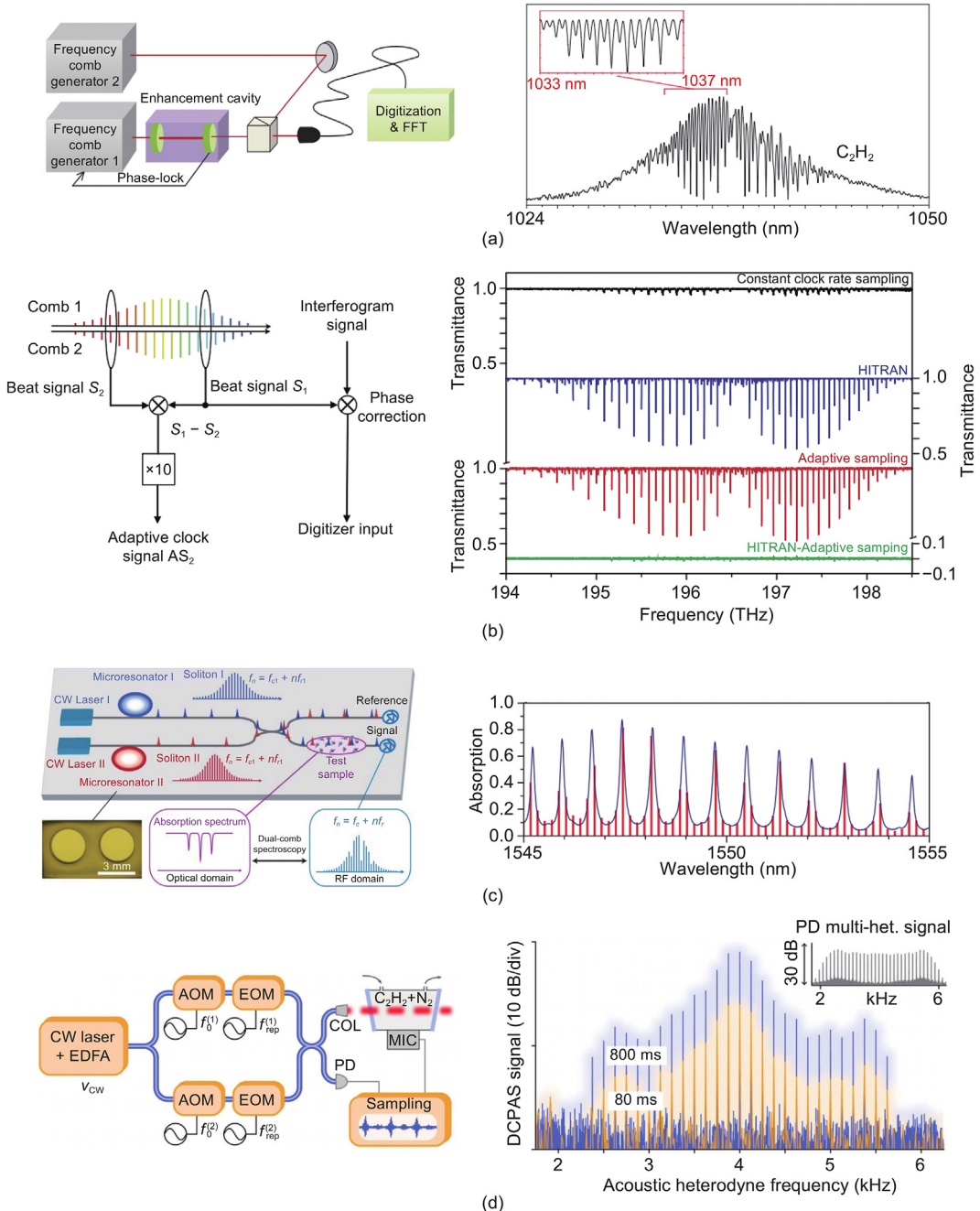


Fig. 9. OFCs for spectroscopy: (a) experimental setup and the measured absorption spectrum of C₂H₂ [110], (b) principle of adaptive DCS and adaptive sampling spectra [111], (c) microresonator-based DCS and measured molecular absorption spectra [112], and (d) experimental setup for the photo-acoustic detection and spectrum of the acoustic multi-heterodyne signal [116].

spurious lines, and without requiring spectral filtering or additional spectral broadening, which provides a new method for Earth-like planet detection and cosmological research.

The quantum frequency comb is a novel field that has recently attracted many researchers. The emergence of quantum OFC realizes the large-scale and precisely controllable systems of the quantum technology, due to its large number of time and frequency modes. And it has achieved very impressive research results. In 2016, Reimer et al. [123] demonstrated that optical integrated Kerr frequency combs could be used to generate several bi- and multi-photon entangled qubits, with direct applications for quantum communications and computation. The two-photon qubits generated on comb lines were symmetric with respect to the pump wavelength and found the

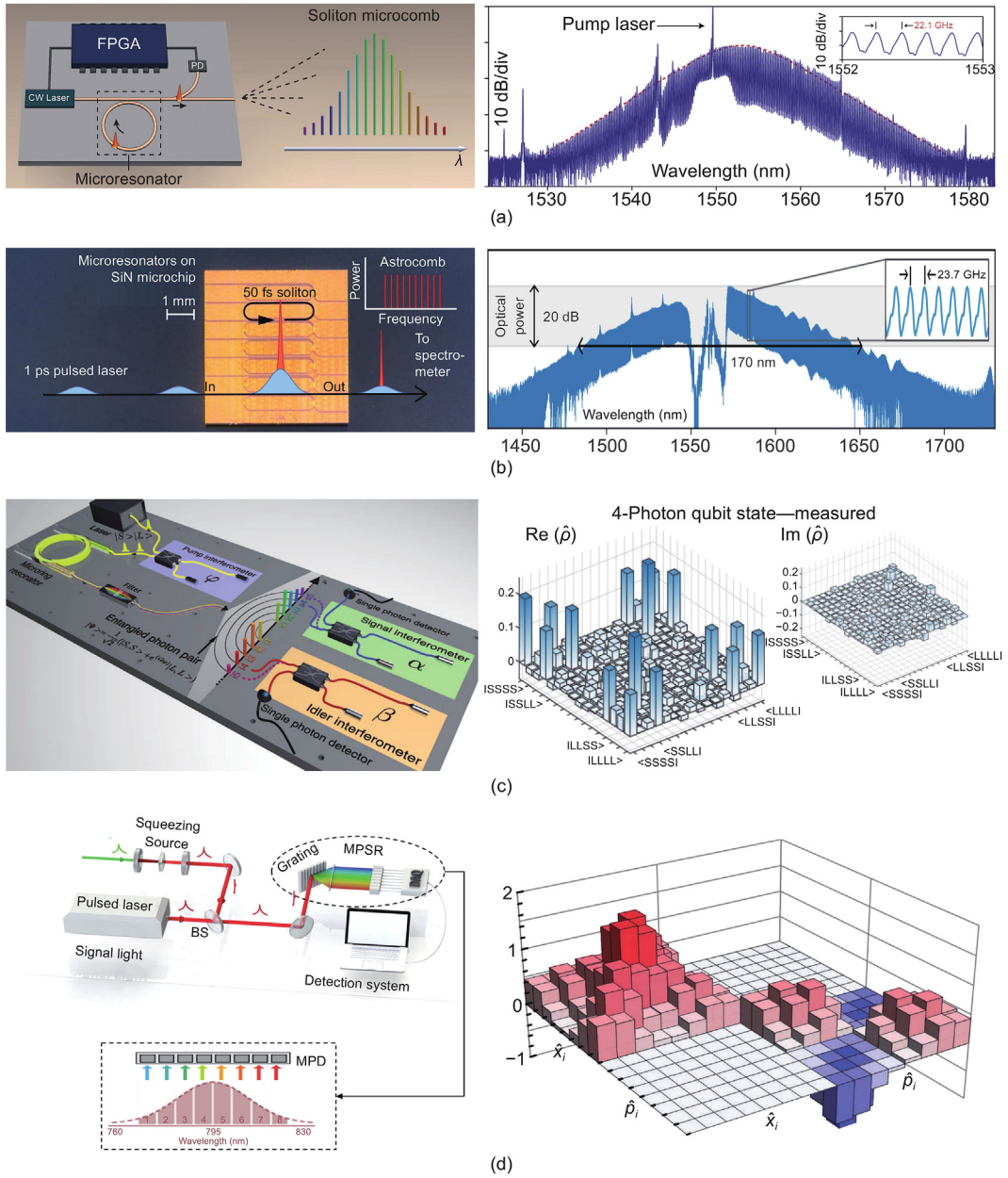


Fig. 10. Astrocombs and quantum frequency combs: (a) concept and optical spectrum of the astrocomb [121], (b) concept of soliton-enabled astrocomb generation and optical spectrum [122], (c) concept of the quantum frequency comb and quantum state characterization [123], and (d) experimental setup and quantum state of the quantum frequency comb [125].

fidelity of 96%, and the four-photon entangled obtained the fidelity of 64%, as shown in Fig. 10 (c). This work provides a scalable and practical platform for optical quantum information processing. In 2020, Wang et al. [124] demonstrated that the parallel quantum key distribution could be achieved using coherent comb lines from the Kerr soliton. This system possesses the advantages of compactness, low cost, robustness, and high efficiency, and will greatly promote the popularization of the quantum key distribution in personal equipment and networks. In 2021, Cai et al. [125] demonstrated single shot multi-parameter estimation of OFC at and beyond the standard quantum limit. The experimental setup and part of the results are shown in Fig. 10 (d). This work provides a proof of the principle for the ability to exceed the standard quantum limit in the measurement of frequency and energy as well as spectral bandwidth fluctuations within OFC. In 2021, Ma et al. [16] demonstrated coherent storage of light in an atomic frequency comb memory over 1 h. And this work might pave the way for large-scale quantum communications based on long-lived solid-state quantum memories.

It should be noted that different applications of OFCs have different FSR requirements. Therefore, it is necessary to tune FSR of OFC to meet different application needs. To date, researchers have proposed a lot of methods to achieve this goal, such as the EO modulation

[126], active mode-locking [127], nonlinear effect [128], amplitude filtering [129], and energy-preserving phase-only manipulation techniques [130].

5. Conclusion and outlook

This article reviews the development, mechanism, generation, regulation, and applications of OFCs which have attracted great attention in recent years. Although OFCs have been applied in many fields, it is still developing rapidly, both in science and engineering.

1) The optical atomic clock technology based on OFCs is a highlighted trend [131]. With the continuous development of the space technology, the synchronization of optical clocks by using OFCs may help to establish a global optical clock network and assist in the synchronization of physical events in different regions, which will be useful for high-precision measurement [132–134].

2) Miniaturization and integration are the keys to the applications of OFCs in the fields of precision handheld micro-/nano-scale devices [48]. But the microcombs integrated on chip commonly require a complicated power supply and control system to make integrated OFC operate properly. Due to the compatibility gap between its chip manufacturing process and heterogeneous CMOS devices, OFCs, control systems, and adaptive feedback systems are still difficult to be integrated all-in-one [56]. Therefore, the development of the next generation of all-chip integrated OFCs with pumping sources and detectors will be a new breakthrough for realizing mass-production and customer-friendly devices [22].

3) Deep learning and artificial intelligence are improving by leaps and bounds. However, the electricity-based calculation speed has reached the bottleneck. Therefore, researchers gradually turned their attention to the faster light. OFCs can be integrated into computer chips and used as high-power-efficiency energy sources for photon calculations. This system is suitable for data parallel processing through wavelength multiplexing [135]. Recent research results show the extraordinary potential of OFCs in the field of photonic computing [136]. With the continuous advancement of the frequency comb technology, it will shine in more fields in the future.

In sum, OFCs will have tremendous development. In terms of production, the performance of OFC can be further improved by combining with materials with fascinating characteristics [137] or designing new structures. In terms of applications, it will develop new instruments with higher performance, higher integration, and broader suitability for various scenarios. For instances, cutting-edge interdisciplinary research that combines OFCs with machine learning [138], quantum science, and other disciplines (such as photonic integrated computing [135,136]) may bring more and more opportunities in the future.

Declaration of competing interest

The authors declare no conflicts of interest.

References

- [1] R. Teets, J. Eckstein, T.W. Hänsch, Coherent two-photon excitation by multiple light pulses, *Phys. Rev. Lett.* 38 (14) (Apr. 1977) 760–764.
- [2] J.N. Eckstein, A.I. Ferguson, T.W. Hänsch, High-resolution two-photon spectroscopy with picosecond light pulses, *Phys. Rev. Lett.* 40 (13) (Mar. 1978) 847–850.
- [3] T. Udem, R. Holzwarth, T.W. Hänsch, Optical frequency metrology, *Nature* 416 (6877) (Mar. 2002) 233–237.
- [4] D.E. Spence, P.N. Kean, W. Sibbett, 60-fsec pulse generation from a self-mode-locked Ti:sapphire laser, *Opt. Lett.* 16 (1) (Jan. 1991) 42–44.
- [5] D.J. Jones, S.A. Diddams, J.K. Ranka, et al., Carrier-envelope phase control of femtosecond mode-locked lasers and direct optical frequency synthesis, *Science* 288 (5466) (Apr. 2000) 635–639.
- [6] W.C. Swann, J.J. McFerran, I. Coddington, et al., Fiber-laser frequency combs with subhertz relative linewidths, *Opt. Lett.* 31 (20) (Oct. 2006) 3046–3048.
- [7] I. Coddington, W.C. Swann, L. Lorini, et al., Coherent optical link over hundreds of metres and hundreds of terahertz with subfemtosecond timing jitter, *Nat. Photonics* 1 (5) (May 2007) 283–287.
- [8] L.A.M. Johnson, P. Gill, H.S. Margolis, Evaluating the performance of the NPL femtosecond frequency combs: agreement at the 10^{-21} level, *Metrologia* 52 (1) (Feb. 2015) 62–71.
- [9] F. Quinlan, F.N. Baynes, T.M. Fortier, et al., Impact of optical amplification and pulse interleaving in low phase noise photonic microwave generation, in: Proc. of CLEO: Science and Innovations, 2014, pp. 1581–1584. San Jose.
- [10] S.A. Diddams, The evolving optical frequency comb [Invited], *J. Opt. Soc. Am. B* 27 (11) (Nov. 2010) B51–B62.
- [11] M.T. Murphy, T. Udem, R. Holzwarth, et al., High-precision wavelength calibration of astronomical spectrographs with laser frequency combs, *Mon. Not. Roy. Astron. Soc.* 380 (2) (Aug. 2007) 839–847.
- [12] M.-X. Tan, X.-Y. Xu, A. Boes, et al., Photonic RF arbitrary waveform generator based on a soliton crystal micro-comb source, *J. Lightwave Technol.* 38 (22) (Nov. 2020) 6221–6226.
- [13] D.A. Braje, M.S. Kirchner, S. Osterman, T. Fortier, S.A. Diddams, Astronomical spectrograph calibration with broad-spectrum frequency combs, *Eur. Phys. J. A* 48 (1) (Jun. 2008) 57–66.
- [14] Y. Geng, X.-T. Huang, W.-W. Cui, et al., Terabit optical OFDM superchannel transmission via coherent carriers of a hybrid chip-scale soliton frequency comb, *Opt. Lett.* 43 (10) (May 2018) 2406–2409.
- [15] R. Zhou, S. Latkowski, J. O’Carroll, R. Phelan, L.P. Barry, P. Anandarajah, 40 nm wavelength tunable gain-switched optical comb source, *Opt. Express* 19 (26) (Dec. 2011) B415–B420.
- [16] Y. Ma, Y.-Z. Ma, Z.-Q. Zhou, C.-F. Li, G.-C. Guo, One-hour coherent optical storage in an atomic frequency comb memory, *Nat. Commun.* 12 (1) (Apr. 2021) 2381, 1–6.
- [17] D.K. Armani, T.J. Kippenberg, S.M. Spillane, K.J. Vahala, Ultra-high-Q toroid microcavity on a chip, *Nature* 421 (6926) (Feb. 2003) 925–928.
- [18] T.J. Kippenberg, S.M. Spillane, K.J. Vahala, Kerr-nonlinearity optical parametric oscillation in an ultrahigh-Q toroid microcavity, *Phys. Rev. Lett.* 93 (8) (Aug. 2004), 083904, 1–4.
- [19] P. Del’Haye, A. Schliesser, O. Arcizet, T. Wilken, R. Holzwarth, T.J. Kippenberg, Optical frequency comb generation from a monolithic microresonator, *Nature* 450 (7173) (Dec. 2007) 1214–1217.
- [20] T. Herr, V. Brasch, J.D. Jost, et al., Temporal solitons in optical microresonators, *Nat. Photonics* 8 (2) (Nov. 2014) 145–152.
- [21] J.S. Levy, A. Gondarenko, M.A. Foster, A.C. Turner-Foster, A.L. Gaeta, M. Lipson, CMOS-compatible multiple-wavelength oscillator for on-chip optical interconnects, *Nat. Photonics* 4 (1) (Jan. 2010) 37–40.
- [22] V. Brasch, M. Geiselmann, T. Herr, et al., Photonic chip-based optical frequency comb using soliton Cherenkov radiation, *Science* 351 (6271) (Jan. 2016)

357–360.

- [23] B.-C. Yao, S.-W. Huang, Y. Liu, et al., Gate-tunable frequency combs in graphene-nitride microresonators, *Nature* 558 (7710) (Jun. 2018) 410–414.
- [24] B.-Q. Shen, L. Chang, J.-Q. Liu, et al., Integrated turnkey soliton microcombs, *Nature* 582 (7812) (Jun. 2020) 365–369.
- [25] T.J. Kippenberg, R. Holzwarth, S.A. Diddams, Microresonator-based optical frequency combs, *Science* 332 (6029) (Apr. 2011) 555–559.
- [26] Y.K. Chembo, N. Yu, Modal expansion approach to optical-frequency-comb generation with monolithic whispering-gallery-mode resonators, *Phys. Rev. A* 82 (3) (Sept. 2010), 033801, 1–18.
- [27] S. Coen, H.G. Randle, T. Sylvestre, M. Erkintalo, Modeling of octave-spanning Kerr frequency combs using a generalized mean-field Lugiato-Lefever model, *Opt Lett.* 38 (1) (Jan. 2013) 37–39.
- [28] M. Karpov, H.-R. Guo, A. Kordts, et al., Raman self-frequency shift of dissipative Kerr solitons in an optical microresonator, *Phys. Rev. Lett.* 116 (10) (Mar. 2016), 103902, 1–5.
- [29] A. Coillet, R. Henriet, P. Salzenstein, K.P. Huy, L. Larger, Y.K. Chembo, Time-domain dynamics and stability analysis of optoelectronic oscillators based on whispering-gallery mode resonators, *IEEE J. Sel. Top. Quant. Electron.* 19 (5) (Sept.–Oct. 2013), 6000112, 1–12.
- [30] G. Ycas, S. Osterman, S.A. Diddams, Generation of a 660–2100 nm laser frequency comb based on an erbium fiber laser, *Opt Lett.* 37 (12) (Jun. 2012) 2199–2201.
- [31] A. Cingöz, D.C. Yost, T.K. Allison, et al., Direct frequency comb spectroscopy in the extreme ultraviolet, *Nature* 482 (7383) (Feb. 2012) 68–71.
- [32] D.M.B. Lesko, H. Timmers, S.-D. Xing, A. Kowlgy, A.J. Lind, S.A. Diddams, A six-octave optical frequency comb from a scalable few-cycle erbium fibre laser, *Nat. Photonics* 15 (4) (Mar. 2021) 281–286.
- [33] Y. Nakajima, H. Inaba, K. Hosaka, et al., A multi-branch, fiber-based frequency comb with millihertz-level relative linewidths using an intra-cavity electro-optic modulator, *Opt Express* 18 (2) (Jan. 2010) 1667–1676.
- [34] C. Erny, K. Moutzouris, T. Biegert, et al., Femtosecond mid-infrared difference-frequency-generation tunable between 3.2 μm and 4.8 μm from a compact fiber source, in: Proc. of Conf. on Lasers and Electro-Optics, Baltimore, 2007, pp. 1138–1140.
- [35] B.R. Washburn, R.W. Fox, N.R. Newbury, et al., Fiber-laser-based frequency comb with a tunable repetition rate, *Opt Express* 12 (20) (Oct. 2004) 4999–5004.
- [36] Y.-S. Liu, J.-G. Zhang, G.-S. Chen, W. Zhao, J. Bai, Low-timing-jitter, stretched-pulse passively mode-locked fiber laser with tunable repetition rate and high operation stability, *J. Opt.* 12 (9) (Sept. 2010), 095204, 1–6.
- [37] Y.J. Kim, B.J. Chun, Y. Kim, S. Hyun, S.W. Kim, Generation of optical frequencies out of the frequency comb of a femtosecond laser for DWDM telecommunication, *Laser Phys. Lett.* 7 (7) (Jul. 2010) 522–527.
- [38] T.R. Schibli, K. Minoshima, F.-L. Hong, et al., An arbitrary optical single-frequency generator based on a femtosecond frequency comb, in: Proc. of Pacific Rim Conf. on Lasers & Electro-Optics, Tokyo, 2005, pp. 1713–1714.
- [39] A.A. Savchenkov, A.B. Matsko, V.S. Ilchenko, I. Solomatin, D. Seidel, L. Maleki, Tunable optical frequency comb with a crystalline whispering gallery mode resonator, *Phys. Rev. Lett.* 101 (9) (Aug. 2008), 093902, 1–4.
- [40] P. Del'Haye, O. Arcizet, A. Schliesser, R. Holzwarth, T.J. Kippenberg, Full stabilization of a microresonator-based optical frequency comb, *Phys. Rev. Lett.* 101 (5) (Aug. 2008), 053903, 1–4.
- [41] P. Del'Haye, A. Coillet, W. Loh, K. Beha, S.B. Papp, S.A. Diddams, Phase steps and resonator detuning measurements in microresonator frequency combs, *Nat. Commun.* 6 (Jan. 2015) 5668, 1–8.
- [42] X. Yi, Q.-F. Yang, K.-Y. Yang, M.G. Suh, K. Vahala, Soliton frequency comb at microwave rates in a high-Q silica microresonator, *Optica* 2 (12) (Dec. 2015) 1078–1085.
- [43] X. Yi, Q.-F. Yang, K.-Y. Yang, K. Vahala, Active capture and stabilization of temporal solitons in microresonators, *Opt Lett.* 41 (9) (May 2016) 2037–2040.
- [44] T.J. Kippenberg, A.L. Gaeta, M. Lipson, M.L. Gorodetsky, Dissipative Kerr solitons in optical microresonators, *Science* 361 (6402) (Aug. 2018), eaan8083, 1–11.
- [45] V. Brasch, M. Geiselmann, M.H.P. Pfeiffer, T.J. Kippenberg, Bringing short-lived dissipative Kerr soliton states in microresonators into a steady state, *Opt Express* 24 (25) (Dec. 2016) 29312–29320.
- [46] Q.-F. Yang, X. Yi, K.-Y. Yang, K. Vahala, Stokes solitons in optical microcavities, *Nat. Phys.* 13 (1) (Jan. 2017) 53–57.
- [47] T. Tan, Z.-Y. Yuan, H. Zhang, et al., Multispecies and individual gas molecule detection using Stokes solitons in a graphene over-modal microresonator, *Nat. Commun.* 12 (1) (Nov. 2021) 6716, 1–8.
- [48] A.L. Gaeta, M. Lipson, T.J. Kippenberg, Photonic-chip-based frequency combs, *Nat. Photonics* 13 (3) (Feb. 2019) 158–169.
- [49] W.-Q. Wang, L.-R. Wang, W.-F. Zhang, Advances in soliton microcomb generation, *Adv. Photon.* 2 (3) (Jan. 2020), 034001, 1–27.
- [50] Z.-Z. Lu, W.-Q. Wang, W.-F. Zhang, et al., Deterministic generation and switching of dissipative Kerr soliton in a thermally controlled micro-resonator, *AIP Adv.* 9 (2) (Feb. 2019), 025314, 1–5.
- [51] C. Joshi, J.K. Jang, K. Luke, et al., Thermally controlled comb generation and soliton modelocking in microresonators, *Opt Lett.* 41 (11) (Jun. 2016) 2565–2568.
- [52] Y. He, Q.-F. Yang, J.-W. Ling, et al., Self-starting bi-chromatic LiNbO₃ soliton microcomb, *Optica* 6 (9) (Sept. 2019) 1138–1144.
- [53] N.G. Pavlov, S. Koptyaev, G.V. Lihachev, et al., Narrow-linewidth lasing and soliton Kerr microcombs with ordinary laser diodes, *Nat. Photonics* 12 (11) (Oct. 2018) 694–698.
- [54] J.-Q. Liu, H. Tian, E. Lucas, et al., Monolithic piezoelectric control of soliton microcombs, *Nature* 583 (7816) (Jul. 2020) 385–390.
- [55] W.-L. Weng, A. Kaszubowska-Anandarajah, J.-J. He, et al., Gain-switched semiconductor laser driven soliton microcombs, *Nat. Commun.* 12 (1) (Mar. 2021) 1425, 1–9.
- [56] A. Pasquazi, M. Peccianti, L. Razzari, et al., Micro-combs : a novel generation of optical sources, *Phys. Rep.* 729 (Jan. 2018) 1–81.
- [57] T. Tan, H.-J. Chen, Z.-Y. Yuan, , et al. January, Gain-assisted chiral soliton microcombs [Online]. Available: <https://arxiv.org/abs/2008.12510v1>, 2020.
- [58] Z.-Z. Lu, H.-J. Chen, W.-Q. Wang, et al., Synthesized soliton crystals, *Nat. Commun.* 12 (1) (May 2021) 3179, 1–7.
- [59] A. Rueda, F. Sedlmeir, M. Kumari, G. Leuchs, H.G.L. Schwefel, Resonant electro-optic frequency comb, *Nature* 568 (7752) (Apr. 2019) 378–381.
- [60] M. Zhang, B. Buscaino, C. Wang, et al., Broadband electro-optic frequency comb generation in a lithium niobate microring resonator, *Nature* 568 (7752) (Mar. 2019) 373–377.
- [61] T. Sakamoto, T. Kawanishi, M. Izutsu, Optimization of electro-optic comb generation using conventional Mach-Zehnder modulator, in: Proc. of Intl. Topical Meeting on Microwave Photonics, Victoria, 2007, pp. 50–53.
- [62] M. Yan, P.-L. Luo, K. Iwakuni, G. Millot, T.W. Hänsch, N. Picqué, Mid-infrared dual-comb spectroscopy with electro-optic modulators, *Light Sci. Appl.* 6 (10) (Apr. 2017), e17076, 1–8.
- [63] A. Parriaux, K. Hammani, G. Millot, Electro-optic frequency combs, *Adv. Opt. Photon.* 12 (1) (Mar. 2020) 223–287.
- [64] M. Brandstetter, C. Deutsch, M. Krall, et al., High power terahertz quantum cascade lasers with symmetric wafer bonded active regions, *Appl. Phys. Lett.* 103 (17) (Oct. 2013), 171113, 1–5.
- [65] A. Danylov, N. Erickson, A. Light, J. Waldman, Phase locking of 2.324 and 2.959 terahertz quantum cascade lasers using a Schottky diode harmonic mixer, *Opt Lett.* 40 (21) (Nov. 2015) 5090–5092.
- [66] A. Hugi, G. Villares, S. Blaser, H.-C. Liu, J. Faist, Mid-infrared frequency comb based on a quantum cascade laser, *Nature* 492 (7428) (Dec. 2012) 229–233.
- [67] L. Consolino, M. Nafa, F. Cappelli, et al., Fully phase-stabilized quantum cascade laser frequency comb, *Nat. Commun.* 10 (1) (Jul. 2019) 2938, 1–7.
- [68] K.-P. Jia, X.-H. Wang, D. Kwon, et al., Photonic flywheel in a monolithic fiber resonator, *Phys. Rev. Lett.* 125 (14) (Oct. 2020), 143902, 1–7.
- [69] C.-Y. Qin, K.-P. Jia, Q.-Y. Li, et al., Electrically controllable laser frequency combs in graphene-fibre microresonators, *Light Sci. Appl.* 9 (1) (Nov. 2020) 185, 1–9.
- [70] Y.-Y. Guo, B. Han, S.-S. Cao, et al., Kilometers long graphene coated optical fibers for fast temperature sensing, in: Proc. of Asia Communications and, Photonics Conf., Beijing, 2021, pp. 1–9.
- [71] H. Hu, L.K. Oxenløwe, Chip-based optical frequency combs for high-capacity optical communications, *Nanophotonics* 10 (5) (Mar. 2021) 1367–1385.
- [72] V. Torres-Company, J. Schröder, A. Fülop, et al., Laser frequency combs for coherent optical communications, *J. Lightwave Technol.* 37 (7) (Apr. 2019) 1663–1670.

- [73] L. Lundberg, M. Karlsson, A. Lorences-Riesgo, et al., Frequency comb-based WDM transmission systems enabling joint signal processing, *Appl. Sci.* 8 (5) (May 2018) 718, 1-25.
- [74] L. Lundberg, M. Mazur, A. Mirani, et al., Phase-coherent lightwave communications with frequency combs, *Nat. Commun.* 11 (1) (Jan. 2020) 201, 1-7.
- [75] E. Temprana, E. Myslivets, B.P.P. Kuo, et al., Overcoming Kerr-induced capacity limit in optical fiber transmission, *Science* 348 (6242) (Jun. 2015) 1445–1448.
- [76] P. Marin-Palomo, J.N. Kemal, M. Karpov, et al., Microresonator-based solitons for massively parallel coherent optical communications, *Nature* 546 (7657) (Jun. 2017) 274–279.
- [77] A. Fülop, M. Mazur, A. Lorences-Riesgo, et al., High-order coherent communications using mode-locked dark-pulse Kerr combs from microresonators, *Nat. Commun.* 9 (1) (Apr. 2018) 1598, 1-8.
- [78] Y. Lu, W.-J. Zhang, B.-X. Xu, X.-Y. Fan, Y.-T. Sun, Z.-Y. He, Directly modulated VCSELs with frequency comb injection for parallel communications, *J. Lightwave Technol.* 39 (5) (Mar. 2021) 1348–1354.
- [79] X.-L. Yan, X.-H. Zou, P.-X. Li, W. Pan, L.-S. Yan, Covert wireless communication using massive optical comb channels for deep denoising, *Photon. Res.* 9 (6) (Jun. 2021) 1124–1133.
- [80] Q.-F. Yang, Q.-X. Ji, L. Wu, et al., Dispersive-wave induced noise limits in miniature soliton microwave sources, *Nat. Commun.* 12 (1) (Mar. 2021) 1442, 1-10.
- [81] H.J. Song, N. Shimizu, T. Furuta, K. Suizu, H. Ito, T. Nagatsuna, Broadband-frequency-tunable sub-terahertz wave generation using an optical comb, AWGs, optical switches, and a uni-traveling carrier photodiode for spectroscopic applications, *J. Lightwave Technol.* 26 (15) (Aug. 2008) 2521–2530.
- [82] W. Liang, D. Eliyahu, V.S. Ilchenko, et al., High spectral purity Kerr frequency comb radio frequency photonic oscillator, *Nat. Commun.* 6 (Aug. 2015) 7957, 1-8.
- [83] E. Lucas, P. Brochard, R. Bouchand, S. Schilt, T. Südmeyer, T.J. Kippenberg, Ultralow-noise photonic microwave synthesis using a soliton microcomb-based transfer oscillator, *Nat. Commun.* 11 (1) (Jan. 2020) 374, 1-8.
- [84] J.-Q. Liu, E. Lucas, A.S. Raja, et al., Photonic microwave generation in the X- and K-band using integrated soliton microcombs, *Nat. Photonics* 14 (8) (Aug. 2020) 486–491.
- [85] Y. Bai, M.-H. Zhang, Q. Shi, et al., Brillouin-Kerr soliton frequency combs in an optical microresonator, *Phys. Rev. Lett.* 126 (6) (Feb. 2021), 063901, 1-7.
- [86] X.-Y. Xu, M.-X. Tan, J.-Y. Wu, et al., Photonic RF and microwave integrator based on a transversal filter with soliton crystal microcombs, in: *IEEE Trans. on Circuits and Systems II: Express Briefs* 67, Dec. 2020, pp. 3582–3586, 12.
- [87] M.-X. Tan, X.-Y. Xu, B. Corcoran, et al., RF and microwave fractional differentiator based on photonics, in: *IEEE Trans. on Circuits and Systems II: Express Briefs* 67, Nov. 2020, pp. 2767–2771, 11.
- [88] T. Fortier, E. Baumann, Author correction: 20 years of developments in optical frequency comb technology and applications, *Commun. Phys.* 3 (1) (May 2020) 85, 1-2.
- [89] Y.-S. Jang, S.W. Kim, Distance measurements using mode-locked lasers: a review, *Nanomanuf. Metrol.* 1 (3) (May 2018) 131–147.
- [90] L.-H. Jia, Y. Wang, X.-Y. Wang, et al., Nonlinear calibration of frequency modulated continuous wave LIDAR based on a microresonator soliton comb, *Opt Lett.* 46 (5) (Mar. 2021) 1025–1028.
- [91] J. Riemsberger, A. Lukashchuk, M. Karpov, et al., Massively parallel coherent laser ranging using a soliton microcomb, *Nature* 581 (7807) (May 2020) 164–170.
- [92] P.O. Schmidt, S. Kimeswenger, H.U. Käufel, A new generation of spectrometer calibration techniques based on optical frequency combs, in: *Proc. of ESO Instrument Calibration Workshop*, 2008, pp. 409–412. Garching.
- [93] G.-C. Wang, Y.-S. Jang, S. Hyun, et al., Absolute positioning by multi-wavelength interferometry referenced to the frequency comb of a femtosecond laser, *Opt Express* 23 (7) (Apr. 2015) 9121–9129.
- [94] G.-C. Wang, L.-T. Tan, S.-H. Yan, Real-time and meter-scale absolute distance measurement by frequency-comb-referenced multi-wavelength interferometry, *Sensors* 18 (2) (Feb. 2018) 500, 1-13.
- [95] Z.-B. Zhu, G.-H. Wu, Dual-comb ranging, *Engineering* 4 (6) (Dec. 2018) 772–778.
- [96] J.-D. Wang, Z.-Z. Lu, W.-Q. Wang, et al., Long-distance ranging with high precision using a soliton microcomb, *Photon. Res.* 8 (12) (Dec. 2020) 1964–1972.
- [97] Y.-S. Jang, H. Liu, J.-H. Yang, M.-B. Yu, D.L. Kwong, C.W. Wong, Nanometric precision distance metrology via hybrid spectrally resolved and homodyne interferometry in a single soliton frequency microcomb, *Phys. Rev. Lett.* 126 (2) (Jan. 2021), 023903, 1-8.
- [98] H. Cao, Y.-J. Song, M.-L. Hu, C. Wang, Singular spectrum analysis for extracting low amplitude vibrations in femtosecond laser time-of-flight distance measurements, *IEEE Photon. J.* 13 (2) (Apr. 2021), 7800110, 1-10.
- [99] Y.-J. Na, C.G. Jeon, C. Ahn, et al., Ultrafast, sub-nanometre-precision and multifunctional time-of-flight detection, *Nat. Photonics* 14 (6) (Feb. 2020) 355–360.
- [100] P. Trocha, M. Karpov, D. Ganin, et al., Ultrafast optical ranging using microresonator soliton frequency combs, *Science* 359 (6378) (Feb. 2018) 887–891.
- [101] M.G. Suh, K.J. Vahala, Soliton microcomb range measurement, *Science* 359 (6378) (Feb. 2018) 884–887.
- [102] S.-Y. Zhou, V. Le, S.-L. Xiong, et al., Dual-comb spectroscopy resolved three-degree-of-freedom sensing, *Photon. Res.* 9 (2) (Feb. 2021) 243–251.
- [103] S.A. van den Berg, S. van Eldik, N. Bhattacharya, Mode-resolved frequency comb interferometry for high-accuracy long distance measurement, *Sci. Rep.* 5 (Sept. 2015), 14661, 1-10.
- [104] H.-Z. Wu, T. Zhao, Z.-Y. Wang, et al., Long distance measurement up to 1.2 km by electro-optic dual-comb interferometry, *Appl. Phys. Lett.* 111 (25) (Dec. 2017), 251901, 1-5.
- [105] Z.-B. Zhu, G.-Y. Xu, K. Ni, Q. Zhou, G.-H. Wu, Synthetic-wavelength-based dual-comb interferometry for fast and precise absolute distance measurement, *Opt Express* 26 (5) (Mar. 2018) 5747–5757.
- [106] B.-C. Yao, Y. Liu, S.-W. Huang, et al., Broadband gate-tunable terahertz plasmons in graphene heterostructures, *Nat. Photonics* 12 (1) (Dec. 2018) 22–28.
- [107] Z.-X. Cao, B.-C. Yao, C.-Y. Qin, et al., Biochemical sensing in graphene-enhanced microfiber resonators with individual molecule sensitivity and selectivity, *Light Sci. Appl.* 8 (1) (Nov. 2019) 107, 1-10.
- [108] N. An, T. Tan, Z. Peng, et al., Electrically tunable four-wave-mixing in graphene heterogeneous fiber for individual gas molecule detection, *Nano Lett.* 20 (9) (Sept. 2020) 6473–6480.
- [109] N. An, C.-Y. Qin, Y.-W. Li, et al., Graphene-fiber biochemical sensors: principles, implementations, and advances, *Photon. Sens.* 11 (1) (Jan. 2021) 123–139.
- [110] B. Bernhardt, A. Ozawa, P. Jacquet, et al., Cavity-enhanced dual-comb spectroscopy, *Nat. Photonics* 4 (1) (Nov. 2010) 55–57.
- [111] T. Ideguchi, A. Poisson, G. Guellachvili, N. Picqué, T.W. Hänsch, Adaptive real-time dual-comb spectroscopy, *Nat. Commun.* 5 (Feb. 2014) 3375, 1-8.
- [112] Q.-F. Yang, M.G. Suh, K.-Y. Yang, X. Yi, K.J. Vahala, Microresonator soliton dual-comb spectroscopy, in: *Proc. of CLEO: Science and Innovations*, 2017, pp. 600–603. San Jose.
- [113] Q.-F. Yang, B.-Q. Shen, H.-M. Wang, et al., Vernier spectrometer using counterpropagating soliton microcombs, *Science* 363 (6430) (Feb. 2019) 965–968.
- [114] M.-J. Yu, Y. Okawachi, A.G. Griffith, N. Picqué, M. Lipson, A.L. Gaeta, Silicon-chip-based mid-infrared dual-comb spectroscopy, *Nat. Commun.* 9 (1) (May 2018) 1869, 1-6.
- [115] T. Lin, A. Dutt, C. Joshi, et al., Broadband ultrahigh-resolution chip-scale scanning soliton dual-comb spectroscopy [Online]. Available: <http://arxiv.org/abs/2001.00869>, 2020.
- [116] T. Wildi, T. Voumard, V. Brasch, G. Yilmaz, T. Herr, Photo-acoustic dual-frequency comb spectroscopy, *Nat. Commun.* 11 (1) (Aug. 2020) 4164, 1-6.
- [117] D.J. Benirschke, N.-R. Han, D. Burghoff, Frequency comb ptychography, *Nat. Commun.* 12 (1) (Jul. 2021) 4244, 1-8.
- [118] C.-Y. Bao, Z.-Q. Yuan, L. Wu, et al., Architecture for microcomb-based GHz-mid-infrared dual-comb spectroscopy, *Nat. Commun.* 12 (1) (Nov. 2021) 6573, 1-8.
- [119] R.A. McCracken, J.M. Charsley, D.T. Reid, A decade of astrocombs: recent advances in frequency combs for astronomy [Invited], *Opt Express* 25 (13) (Jun. 2017) 15058–15078.
- [120] M. Endo, I. Ito, Y. Kobayashi, Direct 15-GHz mode-spacing optical frequency comb with a Kerr-lens mode-locked Yb:Y₂O₃ ceramic laser, *Opt Express* 23 (2) (Jan. 2015) 1276–1282.
- [121] M.G. Suh, X. Yi, Y.-H. Lai, et al., Searching for exoplanets using a microresonator astrocomb, *Nat. Photonics* 13 (1) (Dec. 2019) 25–30.

- [122] E. Obrzud, M. Rainer, A. Harutyunyan, et al., A microphotonic astrocomb, *Nat. Photonics* 13 (1) (Dec. 2019) 31–35.
- [123] C. Reimer, M. Kues, P. Roztocki, et al., Generation of multiphoton entangled quantum states by means of integrated frequency combs, *Science* 351 (6278) (Mar. 2016) 1176–1180.
- [124] F.-X. Wang, W.-Q. Wang, R. Niu, et al., Quantum key distribution with on-chip dissipative Kerr soliton, *Laser Photon. Rev.* 14 (2) (Feb. 2020), 1900190, 1-7.
- [125] Y. Cai, J. Roslund, V. Thiel, C. Fabre, N. Treps, Quantum enhanced measurement of an optical frequency comb, *NPJ Quant. Inform.* 7 (May 2021) 82, 1-8.
- [126] T. Sakamoto, A. Chiba, Multiple-frequency-spaced flat optical comb generation using a multiple-parallel phase modulator, *Opt Lett.* 42 (21) (Nov. 2017) 4462–4465.
- [127] Y. Li, M.-G. Wang, J. Zhang, H.-Q. Mu, C.-C. Wang, F.-P. Yan, Microwave frequency comb generation based on active mode-locking of a polarization-multiplexed dual loop optoelectronic oscillator, in: Proc. of Optical Fiber Communication Conf., 2021, pp. 7–9. Washington.
- [128] J. Fatome, I. El-Mansouri, J.L. Blanchet, et al., Even harmonic pulse train generation by cross-polarization-modulation seeded instability in optical fibers, *J. Opt. Soc. Am. B* 30 (1) (Jan. 2013) 99–106.
- [129] A.M. Weiner, Ultrafast optical pulse shaping: a tutorial review, *Opt Commun.* 284 (15) (Jul. 2011) 3669–3692.
- [130] L.R. Cortés, R. Maram, H.G. de Chatellus, J. Azaña, Arbitrary energy-preserving control of optical pulse trains and frequency combs through generalized Talbot effects, *Laser Photon. Rev.* 13 (12) (Dec. 2019), 1900176, 1-24.
- [131] I. Pupeza, C.-K. Zhang, M. Högnér, J. Ye, Extreme-ultraviolet frequency combs for precision metrology and attosecond science, *Nat. Photonics* 15 (3) (Jan. 2021) 175–186.
- [132] P. Delva, J. Lodewyck, S. Bilicki, et al., Test of special relativity using a fiber network of optical clocks, *Phys. Rev. Lett.* 118 (22) (Jun. 2017), 221102, 1-6.
- [133] P. Del'Haye, A. Coillet, T. Fortier, et al., Phase-coherent microwave-to-optical link with a self-referenced microcomb, *Nat. Photonics* 10 (8) (Jun. 2016) 516–520.
- [134] Z.L. Newman, V. Maurice, T. Drake, et al., Architecture for the photonic integration of an optical atomic clock, *Optica* 6 (5) (May 2019) 680–685.
- [135] J. Feldmann, N. Youngblood, M. Karpov, et al., Parallel convolutional processing using an integrated photonic tensor core, *Nature* 589 (7840) (Jan. 2021) 52–58.
- [136] X.-Y. Xu, M.-X. Tan, B. Corcoran, et al., 11 TOPS photonic convolutional accelerator for optical neural networks, *Nature* 589 (7840) (Jan. 2021) 44–51.
- [137] T. Tan, X.-T. Jiang, C. Wang, B.-C. Yao, H. Zhang, 2D material optoelectronics for information functional device applications: status and challenges, *Adv. Sci.* 7 (11) (Jun. 2020), 2000058, 1-25.
- [138] T. Tan, C. Peng, Z.-Y. Yuan, et al., Predicting Kerr soliton combs in microresonators via deep neural networks, *J. Lightwave Technol.* 38 (23) (Dec. 2020) 6591–6599.



Hao Zhang was born in Shandong in 1997. He received the B.S. degree from University of Electronic Science and Technology of China (UESTC), Chengdu in 2020. He is currently pursuing the M.S. degree with the School of Information and Communication Engineering, UESTC. His research interests include microcavities and microcombs.



Bing Chang was born in Hebei in 1999. She received the B.S. degree from UESTC in 2021. She is currently pursuing the Ph.D. degree with the School of Information and Communication Engineering, UESTC. Her research interest is focused on the applications of optical frequency combs.



Zhao-Yu Li was born in Hebei in 1999. He received the B.S. degree from UESTC in 2021 and the B.S. degree of the 1st honor from University of Glasgow, Glasgow in 2021. He is currently pursuing the M.S. degree with the School of Information and Communication Engineering, UESTC. His research interest is focused on optical computing technology.



Yu-Pei Liang was born in Sichuan in 2000. He is pursuing the B.S. degree with UESTC and is going to pursue his M.S. degree in information and communication engineering in 2022 with UESTC. His research interests include optical sensing and computing.



Chen-Ye Qin was born in Jiangxi in 1997. She received the B.S. degree from UESTC in 2019. She is currently pursuing the M.S. degree with the School of Information and Communication Engineering, UESTC. Her research interests include optical frequency combs and fiber microresonators.



Chun Wang was born in Sichuan in 1996. He received the B.S. degree from Dalian Maritime University, Dalian in 2019. He is currently pursuing the M.S. degree with the School of Information and Communication Engineering, UESTC. His research interests include fiber lasers and fiber laser combs.



Han-Ding Xia received his B.S. and Ph.D. degrees from UESTC in 2009 and 2015, respectively. He is currently an assistant research fellow with the Research Center of Laser Fusion, China Academy of Engineering Physics, Mianyang. His current research interests include fiber lasers and ultrafast laser technology.



Teng Tan is pursuing his Ph.D. degree with UESTC. His main research direction is the excitation and control of optical frequency combs based on the fiber microcavity. He has published more than 6 papers in journals, such as Nature Communications, Advanced Science, Light: Science & Applications, Nano Letters, IEEE-Journal of Lightwave Technology, and Sensors and Actuators B: Chemical, and 6 papers in Conference on Lasers and Electro-Optics, International Conference on Optical Fibre Sensors, and other conferences. He also has authorized 2 patents. He is a student member of IEEE.



Bai-Cheng Yao received his Ph.D. degree in optics engineering from UESTC and University of California, Los Angeles (co-education) in 2016. Then he worked as a research associate with University of Cambridge, Cambridge from 2017 to 2018. He joined UESTC in 2018. He is currently a professor with UESTC. Prof. Yao focuses on the optoelectronic and photonic information devices, especially lasers and sensors. He has published more than 50 papers in journals including Nature, Nature Photonics, Nature Communications, and Nano Letters amongst others, and authorized more than 10 international and domestic patents. He is a member of IEEE, OSA, and SPIE.